Diabetes (2011) 60(3):981-992.

Tubular Injury in a Rat Model of Type 2 Diabetes Is Prevented by Metformin : A Possible Role of HIF-1 α Expression and Oxygen Metabolism

Takiyama, Yumi ; Harumi, Tatsuo ; Watanabe, Jun ; Fujita, Yukihiro ; Honjo, Jun ; Shimizu, Norihiko ; Makino, Yuichi ; Haneda, Masakazu

Tubular Injury in a Rat Model of Type 2 Diabetes Is Prevented by Metformin: A Possible Role of HIF-1α Expression and Oxygen Metabolism

Yumi Takiyama[1], Tatsuo Harumi[2], Jun Watanabe[1], Yukihiro Fujita[1], Jun Honjo[1], Norihiko Shimizu[3], Yuichi Makino[1], and Masakazu Haneda[1]

From the [1]Division of Metabolism and Biosystemic Science, Department of Medicine, [2]Department of Anatomy, [3] Animal Laboratory for Medical Research, Asahikawa Medical University

Midorigaoka higashi 2-1-1-1, Asahikawa 078-8510, Japan.

Running title: METFORMIN INHIBITS HIF-1α EXPRESSION

Address all correspondence and reprint requests to: Yumi Takiyama, MD, PhD.

Division of Metabolism and Biosystemic Science, Department of Medicine, Asahikawa Medical University,

Midorigaoka higashi 2-1-1-1, Asahikawa 078-8510, Japan.

E-mail address: taka0716@asahikawa-med.ac.jp

Telephone number: 81-166-68-2454 Fax number: 81-166-68-2459

the word count of main text: 4000 words

the number of tables and figures: 8 (1 table and 7 figures)

ABSTRACT

OBJECTIVE Chronic hypoxia has been recognized as a key regulator in renal tubulointerstitial fibrosis as seen in diabetic nephropathy (DN), which is associated with activation of hypoxia inducible factor -1α (HIF-1α). We assess here the effects of the biguanide, metformin on the expression of the HIF-1α in DN using renal proximal tubular cells and type2 diabetic rats.

RESEARCH DESIGN AND METHODS We explored the effects of metformin on the expression of HIF-1α using human renal proximal tubular epithelial cells (HRPTECs). Male Zucker diabetic fatty rats (ZDF, Gmi-*fa/fa*) rats were treated from 9 to 39 weeks with metformin (250 mg/kg/day) or insulin.

RESULTS Metformin inhibited hypoxia-induced HIF-1α accumulation and the expression of HIF-1-targeted genes in HRPTECs. Although metformin activated the downstream pathways of AMPK, neither an AMPK activator, AICAR nor the mTOR inhibitor, rapamycin suppressed hypoxia-induced HIF-1α expression. In addition, knockdown of AMPKα did not abolish the inhibitory effects of metformin on HIF-1α expression. The proteasome inhibitor MG-132 completely eradicated the suppression of hypoxia-induced HIF-1α accumulation by metformin. The inhibitors of mitochondrial respiration similarly suppressed hypoxia-induced HIF-1α expression. Metformin

significantly decreased ATP production and oxygen consumption rates, which subsequently leads to increase cellular oxygen tension. Finally, metformin, but not insulin, attenuated tubular HIF-1α expression and pimonidazole staining, and ameliorated tubular injury in ZDF rats.

CONCLUSION Our data suggest that hypoxia-induced HIF-1α accumulation in DN could be suppressed by the antidiabetic drug metformin through the repression of oxygen consumption.

Diabetic nephropathy (DN) is now a leading cause of end-stage renal failure, and therefore constitutes a major portion of progressive kidney disease. Chronic hypoxia and tubulointerstitial fibrosis are presently considered to be a common pathway for various progressive kidney diseases including DN, and hypoxia inducible factor (HIF)-1α plays an important role in these pathological mechanisms (1-4). Recent studies have demonstrated that hypoxia represents an early event in the development and progression of DN (4-6), an increased HIF-1α expression in diabetic kidneys compared to the kidneys of control rats (7) and normal human kidneys (8). In addition, Higgins et al. have demonstrated that HIF-1α enhanced epithelial-to-mesenchymal transition (EMT) in vitro, and that genetic ablation of renal epithelial HIF-1α inhibited the development of tubulointerstitial fibrosis utilizing HIF-1α knockout mice (8). Sun et al. further provided an novel explanation for EMT of hypoxic renal tubular cells through the upregulation of Twist induced by HIF-1α (9). Kimura et al. recently showed that stable expression of HIF-1α in tubular epithelial cells promotes interstitial fibrosis in the knockout mice with von Hippel-Lindau tumor suppressor (VHL), which acts an ubiquitin ligase to promote proteolysis of HIF-α (10).

Metformin has been widely used for treating type 2 diabetes, without the stimulation of insulin production and for this reason it is considered an insulin sensitizer (11). The

UK prospective diabetes study (UKPDS) showed that metformin could reduce macrovascular morbidity and mortality (12), suggesting that it achieved its anti-atherogenic and anti-inflammatory effects by means of antioxidant properties (13). Moreover, metformin significantly decreased the urine albumin excretion rate in patients with type 2 diabetes (14). The benefits of metformin in risk to cardiovascular outcomes and metabolic parameters suggest for its clinical use in chronic kidney disease (15). These precise mechanisms beyond glucose effects of metformin are still obscure. Recently, metformin has been found to activate AMP-activated protein kinase (AMPK), a major cellular regulator of lipid and glucose metabolism (16, 17), via a liver kinase B1 (LKB1)-dependent mechanism (18). LKB1-AMPK -mammalian target of rapamycin (mTOR) pathway is a key regulator of HIF-1- targeted genes and HIF-1-mediated cellular metabolism (19-21). Additionally, a recent study has shown that metformin inhibits insulin and IGF-1-induced HIF-1α expression in non-tumor retinal epithelial ARPE-19 cells (22). These evidences led us to question whether metformin known as an AMPK activator might regulate the expression of HIF-1α protein in renal proximal tubular cells. Therefore, we investigated the effects of metformin on HIF-1α expression using cultured human renal proximal tubular epithelial cells (HRPTECs) and Zucker diabetic fatty rats, a model of type 2 diabetes (23).

RESEARCH DESIGN AND METHODS

Materials. Metformin was provided by Dainippon Sumitomo Pharma, Co. (Japan). 5-aminoimidazole-4-carboxamide ribonucleoside (AICAR), MG-132 and rapamycin were purchased from Calbiochem (San Diego, CA). Anti-AMP-activated protein kinase (AMPK)-α, anti-AMPK-α1, anti-AMPK-α2, anti-phosphorylated (p)-AMPKα (Thr 172), anti-p-acetyl-CoA carboxylase (ACC) (Ser 79), anti-p-mTOR (Ser 2448) antibodies were obtained from Cell Signaling Technology, Inc. (Beverly, MA). The primary antibodies are monoclonal mouse antibodies for human HIF-1α (BD Biosciences, Benford, MA) and for rat HIF-1 α (Novus Biological, Inc, Littleton, CO). D-glucose was purchased from Wako Pure Chemical Industries, Ltd. (Osaka, Japan). ON-TARGETplus SMARTpool siControl (D-001810), AMPKα 1 (NM-006251), AMPKα 2 (NM-006252) small interference RNAs (siRNAs) were purchased from Dharmacon (Lafayette, CO). Alexa Fluor 594 donkey anti-mouse secondary antibody was purchased from Invitrogen (Gaithersburg, MD**).** Other chemicals and antibodies were obtained from Sigma-Aldrich, Inc. (St. Louis, MO), unless otherwise indicated.

Human renal proximal epithelial tubular cell cultures. Human proximal tubular epithelial cells (HPRTEC) were purchased as once- or twice-passaged tubular cells from

Lonza Walkersville, Inc. (Walkersville, MD). The tubular cells were cultured in renal epithelial cell growth medium (REGM) according to the manufacture's instructions, as described before (24). After 24 hrs of starvation with serum-free DMEM, the cells were exposed to reagents under normoxic (21 % O_2) or hypoxic (1 % O_2) conditions for 4~24 h, and were then harvested for experiments. In all experiments were deprived of serum.

RNA isolation, RT-PCR and real-time RT-PCR. Total RNA extraction and cDNA synthesis were preformed as described previously (24). Each cDNA sample was analyzed for gene expression by quantitative real-time PCR with an ABI 7300 Sequence Detector (Applied Biosystems, Foster City, CA) using TaqMan Universal PCR Master Mix (Applied Biosystems) as described previously (24). Unlabelled specific primers were purchased from Applied Biosystems for detecting the human PAI-1(Serpine) gene (Assay ID: HS00167155-ml), human SLC2A1 gene (Assay ID: HS00197884-ml), human HIF-1α gene (Assay ID: HS00153153-ml), human VEGF gene (Assay ID: HS00900054-ml), and 18 S gene (Assay ID: HS 9999991-sl).

siRNAs and HRPTECs transfection. Silencing of AMPKα1, α2 gene expression in HRPTECs was achieved by the siRNA technique, as described previously (24).

Forty-eight hours after transfection, HRPTECs were serum-starved for additional 24 h and subsequently treated as indicated.

Protein extraction and Western blot analysis of intracellular proteins in HRPTECs. Total cellular extracts from HRPTECs were prepared, and Western blot was carried out using a denaturing 8 % Novex tris-glycine gels (Invitrogen Co., Carlsbad, CA) or 10 % NuPage Bis-Tris SDS-PAGE gels under reducing conditions, as described previously (24). Membranes were washed and reprobed with an antibody against α-actinin (Sigma) to control for small variations in protein loading and transfer. Images were acquired using the Adobe^{R} Photoshop program (Adobe Systems Incorporated, San Jose, CA), and processed using Multi Guage (Fuji Film, Tokyo, Japan) for densitometric analysis. Signal intensities in control lanes were arbitrarily assigned a value of 1.00.

Oxygen consumption measurements. Cells were incubated under normoxic (21 % O_2) or hypoxic (1 % O_2) conditions in medium containing 5.5 mM (low) or 25 mM (high) glucose, and then resuspended in normoxic medium. Average oxygen consumption rates in HRPTECs treated with reagents in normoxia or hypoxia for 4 hr were measured in a sealed chamber using a Clark-type electrode.

Measurement of Cell ATP. HRPTECs were incubated with reagents under normoxic or hypoxic conditions for 4 hr. ATP production was monitored by glucose-6-phosphate formation. Briefly, cells were extracted with perchloric acid (6 %), centrifuged (8000x g, 10 min). Subsequently, the extract was neutralized with K_2CO_3 (5 M) neutralized to pH 7. $NADP^+$ (0.5 mM) and glucose 6-phosphate dehydrogenase (0.25 U) were then added and ATP production was monitored from NADPH content by spectrophotometry at 340 nm. Cell protein was determined in parallel dishes for the normalization of the ATP values.

Imaging of reactive oxygen species. The oxidative fluorescent dihydroethidium (DHE) (Sigma) was used to evaluate intracellular production of superoxide (O_2^-) (25). In brief, cells after incubation overnight with or without 1 mM metformin or 1 mM AICAR under normoxic and hypoxic conditions were washed with serum-free and phenol-red-free DMEM and loaded with 5 μM DHE. After incubation for 10 min in the dark, the cells were washed with PBS and were subjected to fluorescence microscopy.

NADPH content. NADPH content was determined using NADP/NADPH

Quantification kit (BioVision, Mountain View, CA) and the protocol supplied by the manufacturer.

Immunocytochemistry. HRPTEC were cultured on four-chamber glass slides (BD Biosciences) to reach 80 % confluence. After exposure to 1 mM metformin or 1 mM AICAR for 4 h under normoxic or hypoxic conditions, the cells were fixed with 100 % ethanol for 10 min, cells were incubated with an anti-HIF-1α antibody (1:100, BD Biosciences) at 4 C overnight. Then, cells were rinsed in PBS and subsequently incubated with Alexa Fluor 594 donkey anti-mouse secondary antibody (Invitrogen) at 1: 200 dilution overnight at 4 C. Finally, slides were analyzed by cofocal laser scanning microscopy.

Detection of cellular hypoxia. Cellular hypoxia was detected by adding pimonidazole hydrochloride (200 mmol/L; Hypoxyprobe-1, Hydroxyprobe. Inc., Burlington, MA), which binds to cells or tissues with pO_2 levels below 10 mmHg, to HRPTEC that were treated with 1 mM metformin or 1 mM AICAR, and exposed to hypoxia (1% O_2) for 4 hours. To detect hypoxic conditions in each group of rats, pimonidazole (60 mg/kg) was injected intraperitoneally 1 hour before sacrifice. Staining

was performed according to the manufacturer's instructions.

Animals. Male Zucker diabetic fatty rats (ZDF/Gmi-*fa/fa*) and their heterozygous (ZDF/Gmi-+/*fa*) lean littermates were purchased from Charles River Japan, Inc. Animals purchased at 7 weeks of age were administered were given an ad libitum commercial pellet diet CE-2 (CLEA Japan), and tap water. ZDF rats were randomly assigned to four groups at the age of 9 weeks. A first group did not receive an active pharmacological treatment and were used as a control (ZDF control). A second group received metformin in standard chow at a concentration of 3.3 g/kg (ZDF+M). Taking into account an average daily food intake of 32.4 g/rat, a dose approximately 253.2 $mg \cdot kg^{-1} \cdot day^{-1}$ was achieved. The metformin dose is compatible to those used in previous studies in rats (26, 27). A third group was treated with sustained release insulin implant (~2U/day/implant) (Lin Shin Canada, Ontario, Canada: ZDF+I). Heterozygous animals without active treatment were used as non-diabetic, lean controls (ZL). Tail post-prandial glucose in whole blood was quantified using a glucose analyzer One touch (Life Scan, Johnson & Johnson Co., Milpitas, CA). Hemoglobin A1c (A1c) was measured using the DCA 2000 analyzer (Siemens Medical Solutions Diagnostics, Tokyo, Japan). Renal function was assessed by measuring urinary albumin excretion.

Urinary albumin was quantified using the Nephrat kit (Exocell, Philadelphia, PA) according to manufacturer's instructions. Animals were killed at the age of 17 weeks for pimonidazole staining, and at the age of 39 weeks for assessment of morphology and immunohistochemistry for HIF-1α by over anesthetization with isoflurane and cardiac puncture. The kidneys were fixed with perfusion as described in a previous study (28). The Research Center for Animal Life Science of Asahikawa Medical College approved all experiments.

Morphological analysis and immunohistochemistry. To evaluate HIF-1α or pimonidazole expression in the kidney, immunohistochemistry was performed with mouse monoclonal anti-HIF-1α antibody (ESEE 122, 1:100) or mouse anti-pimonidazole (1:1000), as described previously (24). The positive immunoreactivity for nuclear HIF-1α protein or cytosolic pimonidazole was estimated as absent (0) for negative, low (1) for positive immunoreactivity for 1-20 %, intermediate (2) for 21-50% and high (3) for more than 50% of the tubular cells in the juxtamedullary cortical and outer medullar regions. Assessment of tubulointerstitial injury was evaluated in the juxtamedullary cortical and outer medullar regions using periodic acid-Schiff (PAS) stain staining and a semiquantitative scoring system

evaluating interstitial fibrosis, inflammation, tubular atrophy, tubular dilation, debris accumulation, and cast formation. A score of 0 means normal tubulointerstitium, 1 means injury in less than 25 %, 2 means injury in up to 50 %, and 3 means injury in more than 50 % of the biopsy specimen.

Statistical analysis. Three separate experiments at least were performed per protocol. Each treatment group was assayed in duplicate for real-time RT-PCR. The values shown represent the means ± SD. Statistical analysis was performed by ANOVA and Bonferroni post hoc test. Values of $P < 0.05$ were considered statistically significant.

RESULTS

Metformin inhibits hypoxia-induced HIF-1α protein accumulation. We investigated the impact of metformin on hypoxia-induced HIF-1α expression. HRPTECs faintly expressed HIF-1α protein under normoxic condition (Fig. 1 *A*). The treatment of hypoxia (1% O_2) markedly induced HIF-1α protein accumulation in HRPTECs, and metformin at the concentration of 1 mM inhibited hypoxia-induced HIF-1α protein expression (Fig. 1*A*). Densitometric analysis showed that hypoxia significantly induced HIF-1α protein expression compared to the control in normoxia ($p<0.01$), and a significant approximately 85 % attenuation in hypoxia-induced HIF-1α protein accumulation in HRPTECs treated with 1 mM metformin, compared to hypoxia-treated controls ($p<0.01$) (Fig. 1*B*). The inhibitory effect of metformin was detected at the concentration of 10 μM which was therapeutic concentration as described in previous studies (11, 29) (Fig. 1*C, D*), and for the incubation time of 4~24 hr (data not shown). In contrast, HIF-1α mRNA levels were not reduced by metformin in hypoxia, suggesting that metformin decreased HIF-1α protein via posttranslational mechanisms (Fig. 1 *E*).

Metformin inhibits hypoxia-induced PAI-1, VEGF and Glut-1 mRNA expressions.

We examined the effects of metformin on the expression of HIF-1 target genes in HRPTECs (Fig. 1*F-H*). Real-time PCR results showed that hypoxia significantly promoted PAI-1, VEGF, and Glut-1 gene expression in HRPTECs. Treatment with 10 mM metformin significantly reduced the enhancing effects of hypoxia on these mRNA expressions.

Metformin inhibits hypoxia-induced HIF-1α expression independent of AMPK. As shown in Fig.1*A&C*, metformin inhibited hypoxia-induced HIF-1α protein accumulation in HRPTECs, accompanied by increased AMPKα phosphorylation. We also determined the effects of an AMPK activator, AICAR, on hypoxia-induced HIF-1α expression (Fig.1*A*). Although AICAR stimulated the phosphorylation of AMPK and ACC and inhibited the phosphorylation of mTOR like metformin under normoxic and hypoxic conditions, AICAR failed to suppress hypoxia-induced HIF-1α expression (Fig. *1A*). To study the role of AMPK on inhibitory effects of metformin on HIF-1α expression, we have taken a genetic approach to inhibit the AMPK activity under hypoxic condition. Immunoblots using anti-phosphorylated (Thr172)-AMPKα1 and α2 antibody increased significantly in response to metformin dose-dependently in siAMPKα1-treated cells, suggesting that the presence of AMPKα_2 compensated for the

absence of AMPKα_1 (Fig. 2*A*). In contrast, total p-AMPKα content was markedly suppressed in siAMPKα2-transfected cells treated with metformin (Fig. 2*C*), indicating that metformin could predominantly augment the phosphorylation of AMPKα_2 in HRPTECs, which was consistent with the previous study investigating the effects of AICAR, hypoxia and rotenone on isoform-specific AMPK activity (30). Thus, lowering the AMPKα protein using specific siRNA for AMPKα1 or α2 did not affect hypoxia-induced HIF-1α expression and failed to abolish the inhibitory effects of metformin on hypoxia-induced HIF-1α expression (Fig. 2*A*-*D*).

The proteasomal inhibitor MG-132 pretreatment restores the inhibitory effects of metformin on hypoxia-induced HIF-1α expression. To examine the post-translational regulation of HIF-1α protein by metformin, we used the proteasomal inhibitor MG-132. As shown in Fig. 2*E*, MG-132 restored the inhibitory effect of metformin on hypoxia-induced HIF-1α accumulation, indicating that metformin exhibited its inhibitory effect on HIF-1α accumulation by promoting proteasomal HIF-1α degradation. Whereas, an AMPK inhibitor, compound C (20 μM) failed to antagonize the inhibitory effect of metformin on HIF-1α protein expression (Fig.2*E*).

High glucose does not affect the inhibitory effects of metformin on hypoxia-induced HIF-1α expression. As shown in Fig. 3*A*, high glucose attenuated the stimulatory effects of metformin on the phosphorylation of AMPKα and ACC, and restored the inhibitory effect of metformin on p-mTOR expression. These results were similar to those of a recent study in diabetic rats (31). However, the treatment of high glucose did not blunt the inhibitory effect of metformin on HIF-1α expression (Fig. 3 *A*, *B*), concomitantly suggesting that the activation of AMPKα is insufficient for the inhibitory effect of metformin on hypoxia-induced HIF-1α expression.

Mitochondrial respiratory complex inhibitors, but not rapamycin, mimic the actions of metformin on AMPK activation and hypoxia-induced HIF-1α expression. To determine the mechanism implicated in the regulation of HIF-1α expressions in HRPTECs, subsequent experiments were achieved by the use of inhibitors of mitochondrial pyruvate transport (α-cyano-4-hydroxycinnamate; CHC, 0.1 mM), mTOR (rapamycin, 100 nM), mitochondrial respiratory complex I (rotenone, 0.25 μM, 25 μM), and mitochondrial respiratory complex III (antimycin A, 10 ng/ml, 1 μg/ml). The expression of HIF-1α induced by hypoxia was unaffected by CHC and rapamycin (Fig.4*A*), whereas it was completely blocked by rotenone and antimycin A (Fig.4*B*).

Moreover, rotenone and antimycin A increased the phosphorylation of AMPKα and ACC, and decreased the expression of p-mTOR (Fig. 4*B*).

Metformin decreased oxygen consumption and intracellular ATP levels. Having identified that metformin had the similar effects on the expressions of hypoxia-induced HIF-1α protein and AMPK as mitochondrial respiratory inhibitors, we then directly measured the oxygen consumption and intracellular ATP levels in HRPTECs treated with 1 mM metformin and 1 mM AICAR under normoxic and hypoxic conditions in medium containing 5.5 mM (low) or 25 mM (high) glucose for 4 hr. As shown in Fig. 4*C*, hypoxia decreased oxygen consumption down to 76.5 % of the control in normoxia, which was consistent with the previous study (32), while this response to hypoxia was blunted by the treatment of 25 mM glucose (Fig. 4*D*). Notably, metformin significantly inhibited oxygen consumption to less than 50 % of controls, independent of the oxygen conditions or the glucose milieu (Fig. 4 *C*, *D*). In addition, the results show that cell ATP was trend to decrease during metformin treatment under either normoxic or hypoxic conditions in contrast to the enhancement of ATP levels by the treatment of AICAR (Fig. 4*E*). Consistent with a previous study (33), hypoxia did not induced ATP depletion in HRPTEC, because the metabolic might shift to anaerobic glycolysis seems to have been

sufficient to maintain ATP in hypoxic cells (Fig. 4*E*). In contrast, 25 mM glucose attenuated ATP levels and the inhibitory effects of metformin on ATP levels in either normoxia or hypoxia (Fig. 4*F*).

DPI, but not NAC, mimics the effects of metformin on AMPKα and mTOR phosphorylation, and on hypoxia-induced HIF-1α expression. Furthermore, we examined the effects of the NADPH oxidase inhibitors diphenylene iodonium (DPI, 10 μM) and antioxidant, N-acetylcysteine (NAC, 5 mM) on the expression of HIF-1α and the phosphorylation of AMPKα and mTOR under normoxic and hypoxic conditions for 4 h. DPI, but not NAC, inhibited hypoxia-induced HIF-1α expression, increased the phosphorylation of AMPKα, ACC, and decreased the phosphorylation of mTOR (Fig. 5*A*). Although DPI has been also known to inhibit mitochondrial complex I (34, 35), we measured NADPH content in order to evaluate whether the inhibition of NADPH oxidase by metformin was involved in the inhibitory effects of metformin on HIF-1α expression. Both metformin and AICAR recovered hypoxia-decreased NADPH content, suggesting that inhibition of NADPH oxidase could not be due to the inhibitory effect of metformin.

Effects of metformin on reactive oxygen species (ROS) production in HRPTECs.

To investigate whether ROS production may be implicated in the inhibitory effects of metformin on HIF-1α expression, DHE staining was examined in HRPTECs. As shown in Fig. 5*C* upper panel, hypoxia decreased DHE-associated fluorescence in low glucose medium compared to that under normoxic conditions. In the medium containing low glucose, metformin increased DHE staining independent of oxygen tension as reported in the previous study (36), in contrast to AICAR (Fig. 5*C*). High glucose enhanced ROS production compared with low glucose, and metformin decreased high-glucose induced ROS production especially in normoxia (Fig. 5*C* lower panel). Thus, these observations suggested that intracellular ROS production was not involved in the inhibitory effect of metformin on HIF-1α expression.

Metformin restored hypoxic conditions

Because metformin decreased oxygen consumption in HRPTECs, we investigated whether metformin increases intracellular oxygen tension using a hypoxia-sensitive dye, pimonidazole (Fig.5*D*). Notably, metformin, but not AICAR, rescued hypoxic state in HRPTECs under hypoxic conditions. In addition, immunocytochemical analysis confirmed that hypoxia apparently induced the nuclear expression of HIF-1α in

HRPTECs compared to those in normoxia, and metformin inhibited hypoxia-induced HIF-1α nuclear stainings (Fig. 5*D*). AICAR did not evidently alter the expression of HIF-1α in HRPTECs under hypoxic conditions (Fig. 5*D*). We also examined the effects of metformin on the state of hypoxia in the kidney (Fig.6*A*, *B*). Intensity of pimonidazole staining was increased in tubular cells of the kidney cortex of ZDF, which was significantly attenuated by metformin, but not by insulin.

Metformin suppressed tubular HIF-1α expression in type 2 diabetic rats. To confirm the effects of metformin on tubular HIF-1α expression *in vivo*, we treated ZDF rats with metformin for 30 weeks. As expected, ZDF rats were hyperglycemic, and administration of metformin to ZDF rats significantly decreased HbA1c by 24 % ($p<0.01$) (Table 1). ZDF rats had increased urinary volume out and albumin excretion compared with lean control as described previously (23). Treatment of ZDF rats with metformin significantly prevented an increase in urinary albumin excretion to 58.3 % of ZDF rats ($p<0.05$) (Table 1). Consistent with the lack of albuminuria, ZL rats as lean controls showed neither glomerulosclerosis nor tubular injury (Fig. 6*C. d, e*). ZL rats exhibited the immunostainings of HIF-1α only in the inner medullar tubules (Fig. 6*C. b*). Intriguingly, ZDF rats showed strong nuclear HIF-1α expressions, especially in outer

medullar and cortical proximal tubules in addition to the inner medulla (Fig. 6*C. f-h*), which is consistent with previous data in human diabetic kidney (8) and in the kidney of STZ-induced diabetic rats (7). In addition, kidneys of ZDF rats showed glomerulosclerosis and tubulointerstitial injuries as described before (23) (Fig. 6*C. i, j*). Notably, positive immunostaining for HIF-1α was evidently decreased in kidneys of metformin treated ZDF rats (Fig. 6*C. k, m*), accompanied by amelioration of the tubular injury (Fig. 6*C. n, o*) , which was contrast to those in kidneys of insulin-treated rats as described in the previous study (37) (Fig.6*C. p, r, s, t*). Semiquantitative assessment for HIF-1α immunostaining and injury in cortical and outer medullary tubules revealed that chronic metformin treatment significantly decreased HIF-1α expression, and ameliorated tubular injury in ZDF rats (Table 1).

DISCUSSION

In this study, we have found that metformin inhibits hypoxia-induced HIF-1α protein expression and thus the expression of its targeted genes, probably via the inhibition of mitochondrial respiration in HRPTECs.

Metformin has been found to activate AMPK, a major cellular regulator of lipid and glucose metabolism (16-18). Previous studies have also shown that metformin is an inhibitor of complex I of the mitochondrial respiratory chain (38, 39), independent of AMPK pathway (40, 41).

To investigate the underlying mechanism(s) of the action of metformin, we first have assessed the role of AMPK activation in hypoxia-induced HIF-1α expression, utilizing AICAR**,** Compound C and siRNA for AMPK-α1, or -α2. We find that metformin-induced AMPK phosphorylation is not related to HIF-1α inhibition. In addition, we show that metformin suppresses mitochondrial respiratory function suggesting that the redistribution of intracellular oxygen is involved in the inhibitory effects of metformin on HIF-1α expression as described in a previous study (42). Collectively, our results suggest that metformin inhibits HIF-1α expression through the suppression of mitochondrial respiration described as inhibition of oxygen consumption and intracellular ATP levels, which subsequently activates AMPK pathways, proposing

that AMPKα is a downstream regulator of the mitochondrial respiratory chain. That is probably the reason that an AMPK activator, AICAR, fails to inhibit hypoxia-induced HIF-1α expression.

AMPK activated by metformin has been reported to increase glucose transporter (GLUT-1 and GLUT-4) and glycolytic enzymes, thereby enhancing glycolytic glucose utilization (43), and to directly stimulate glycolysis in hypoxic or anoxic cells (44). Thus, metformin could promote Pasteur effects, which include decreased oxidative phosphorylation and an increase in anaerobic fermentation (45), by inhibiting mitochondrial respiration and increasing glucose uptake mediated by AMPK activation. Although metformin inhibits hypoxia-induced Glut-1 expression in HRPTECs, an HIF-1α mediated increase in glucose uptake and metabolism during severe hypoxia is known not to be required for cell survival using cultured mouse primary renal proximal tubular cells (33). Intriguingly, high glucose increases oxygen consumption even under hypoxic conditions, but fails to augment the ATP production, indicating that high glucose abolishes Pasteur effects which are adaptive responses to hypoxic stress and that high glucose decreases mitochondrial efficiency by uncoupling oxygen consumption from ATP production. HIF-1-dependent block to oxygen utilization results in increased oxygen availability, decreased cell death when total

oxygen is limiting (32). Therefore, our findings suggest that, in chronic hypoxia as seen in DN, metformin may rescue the renal proximal tubular cells from hypoxia, oxidative stress and energy depletion by suppressing oxygen consumption via inhibition of mitochondrial respiratory chain complex I, instead of HIF-1, subsequently restore Pasteur effects which are impaired by hyperglycemia (Fig.7).

In chronic kidney injury including DN, hypoxia promotes the development of renal fibrosis by inducing CTGF (46) and EMT (8, 9, 47) through a HIF-1-dependent pathway in renal tubular cells by augmenting apoptosis of glomerular endothelial cells (48) and by upregulating matrix production and decreasing turnover in renal fibroblasts (49). Very recently, Kimura et al. induced interstitial fibrosis in the kidney of aged $VHL^{-/-}$ mice, in which pronounced HIF-1α expression was observed in cortical tubular epithelial cells (10). They also demonstrated that the anti-HIF-1α agent [3-(5'-hydroxymethyl-2'-furyl)-1-benzyl indazole] (YC-1) ameliorated interstitial fibrosis in unilateral obstruction kidneys (10). We have shown that a preclinical study using ZDF rats confirmed the expression of HIF-1α in DN, which has been described as the presence of hypoxia in previous studies (4-8), and explore the renoprotective effects of metformin *in vivo*.

In conclusion, these results *in vitro* and *in vivo* indicate for the first time that

the anti-diabetic drug metformin inhibits renal tubular HIF-1α expression. These data provide a novel mechanism of effects of metformin to improve microalbuminuria in DN (14), protecting from hypoxia-induced renal fibrosis by attenuating the expression of HIF-1α (Fig.7).

AUTHOR CONTRIBUTIONS

Y.T. researched data, wrote manuscript. T.H. contributed to discussion. J.W. researched data. Y.F. researched data. J.H. researched data. N.S. contributed to discussion. Y.M. contributed to discussion. M.H. contributed to discussion, reviewed/edited manuscript.

ACKNOWLEDGMENTS

The authors are grateful to Ken Inoki (University of Michigan, Ann Arbor) and Shin-ichi Araki (Shiga University of Medical Science) for helpful discussions. We also express our appreciation to Shinji Kume (Shiga University of Medical Science) for his technical assistance.

No potential conflicts of interest relevant to this article were reported.

REFERENCES

1. Nangaku M. Chronic hypoxia and tubulointerstitial injury: a final common pathway to end-stage renal failure. *J Am Soc Nephrol* 2006; 17: 17-25
2. Haase VH. The VHL/HIF oxygen-sensing pathway and its relevance to kidney disease. *Kidney Int* 2006; 69:1302-1307
3. Eckardt KU, Bernhardt W, Willam C, Wiesener M. Hypoxia-inducible transcription factors and their role in renal disease. *Semin Nephrol* 2007; 27: 363-372
4. Singh DK, Winocour P, Farrington K. Mechanisms of disease: the hypoxic tubular hypothesis of diabetic nephropathy. *Nat Clin Prac Neph* 2008; 4: 216-228
5. Ries M, Basseau F, Tyndal B, Jones R, Deminière C, Catargi B, Combe C, Moonen CW, Grenier N. Renal diffusion and BOLD MRI in experimental diabetic nephropathy. Blood oxygen level-dependent. *J Magn Reson Imaging* 2003; 17: 104-113.
6. Palm F, Hansell P, Ronquist G, Waldenström A, Liss P, Carlsson PO. Polyol-pathway-dependent disturbances in renal medullary metabolism in experimental insulin deficient diabetes mellitus in rats. *Diabetologia* 2004; 47: 1223–1231
7. Rosenberg C, Khamaisi M, Abassi Z, Shilo V, Weksler-Zangen S, Goldfarb M, Shina A, Zibertrest F, Eckardt K-U, Rosen S, Heyman SN: Adaptation to hypoxia in the diabetic rat kidney. *Kidney Int* 2008; 73:34-42
8. Higgins DF, Kimura K, Bernhardt WM, Shrimanker N, Akai Y, Hohenstein B, Saito Y, Johnson RS, Kretzler M, Cohen CD, Eckardt KU, Iwano M, Haase VH. Hypoxia promotes fibrogenesis in vivo via HIF-1 stimulation of epithelial-to-mesenchymal transition. *J Clin Invest* 117: 3810-3820
9. Sun S, Ning X, Zhang Y, Lu Y, Nie Y, Han S, Liu L, Du R, Xia L, He L, Fan D. Hypoxia-inducible factor-1α induces Twist expression in tubular epithelial cells subjected to hypoxia, leading to epithelial-to-mesenchymal transition. *Kidney Int* 2009; 75: 1278-1287
10. Kimura K, Iwano M, Higgins DF, Yamaguchi Y, Nakatani K, Harada K, Kubo A, Akai Y, Rankin EB, Neilson EG, Haase VH, Saito Y. Stable expression of HIF-1α in tubular epithelial cells promotes interstitial fibrosis. *Am J Physiol Renal Physiol* 2008; 295:F1023-F1029
11. Bailey CJ, Turner RC. Metformin. *New Engl J Med* 1996; 334:574-579

12. UK Prospective Diabetes Study (UKPDS) Group. Effect of intensive blood-glucose control with metformin on complications in overweight patients with type 2 diabetes (UKPDS 34). *Lancet* 1998; 352: 854-865
13. Abbasi F, Chu JW, McLaughlin T, Lamendola C, Leavy ET, Reaven GM. Effect of metformin treatment on multiple cardiovascular disease risk factors in patients with type 2 diabetes mellitus. *Metabolism* 2004; 53: 159-164
14. Amador-Licona N, Guizar-Mendoza JM, Vargas E, Sanchez-Camargo G, Zamora-Mata L. The short-term effect of a switch from glibenclamide to metformin on blood pressure and microalbuminuria in patients with type 2 diabetes mellitus. *Arch Med Res* 2007; 31: 571-575
15. Pilmore H. Review: Metformin: potential benefits and use in chronic kidney disease. *Nephrology* 2010; 15: 412-418
16. Zhou G, Myers R, Li Y, Chen Y, Shen X, Fenyk-Melody J, Wu M, Ventre J, Doebber T, Fujii N, Musi N, Hirshman MF, Goodyear LJ, Moller DE. Role of AMP-activated protein kinase in mechanism of metformin action. *J Clin Invest* 2001; 108: 1167-1174
17. Hawley SA, Gadalla AE, Oslen GS, Hardie DG. The antidiabetic drug metformin activates the AMP-activated protein kinase cascade via an adenine nucleotide-independent mechanism. *Diabetes* 2002; 51: 2420-2425
18. Shaw RJ, Lamia KA, Vasquez D, Koo SH, Bardeesy N, DePinho RA, Montminy M, Cantley LC. The kinase LKB1 mediates glucose homeostasis in liver and therapeutic effects of metformin. *Science* 310:1642–1646, 2005
19. Lee M, Hwang JT, Lee HJ, Jung SN, Kang I, Chi SG, Kim SS, Ha J. AMP-activated protein kinase activity is critical for hypoxia-inducible factor-1 transcriptional activity and its target gene expression under hypoxic conditions in DU 145 cells. *J Biol Chem* 2002; 278: 39653-39661
20. Shackelford DB, Vasquez DS, Corbeil J, Wu S, Leblanc M, Wu CL, Vera DR, Shaw RJ. mTOR and HIF-1alpha-mediated tumor metabolism in an LKB1 mouse model of Peutz-Jeghers syndrome. *Proc Natl Acad Sci U S A* 2009; 106: 11137-11142
21. Lieberthal W, Levine JS. The role of the mammalian target of rapamycin (mTOR) in renal disease. *J Am Soc Neprhol* 2009; 20: 2493-2502
22. Treins C, Murdaca J, Van Obberghen E, Giorgetti-Peraldi S. AMPK activation inhibits the expression of HIF-1alpha induced by insulin and IGF-1. *Biochem Biophys Res Commun* 2006; 342: 1197-202

23. Coimbra TM, Janssen U, Grone HJ, Ostendorf T, Kunter U, Schmidt H, Floege J. Early events leading to renal injury in obese Zucker (fatty) rats with type II diabetes. *Kidney Int* 2000; 57: 167-182
24. Miyauchi K, Takiyama Y, Honjyo J, Tateno M, Haneda M. Upregulated IL-18 expression in type 2 diabetic subjects with nephropathy: TGF-beta1 enhanced IL-18 expression in human renal proximal tubular epithelial cells. *Diabetes Res Clin Pract* 2009; 83: 190-199
25. Bindokas VP, Jordan J, Lee CC, Miller RJ. Superoxide production in rat hippocampal neurons: selective imaging with hydroethidine. *J Neuroscie* 1996; 16: 1324 -1336
26. Smith AC, Mullen KL, Junkin KA, Nickerson J, Chabowski A, Bonen A, Dyck DJ. Metformin and exercise reduce muscle FAT/CD36 and lipid accumulation and blunt the progression of high-fat diet-induced hyperglycemia. *Am J Physiol Endocrinol Metab* 2007; 293: E172-E181
27. Cleasby ME, Dzamko N, Hegarty BD, Cooney GJ, Kraegen EW, Ye JM. Metformin prevents the development of acute lipid-induced insulin resistance in the rat through altered hepatic signaling mechanisms. *Diabetes* 2004; 53: 3258-3266
28. Deji N, Kume S, Araki S, Soumura M, Sugimoto T, Isshiki K, Chin-Kanasaki M, Sakaguchi M, Koya D, Haneda M, Kashiwagi A, Uzu T. Structural and functional changes in the kidneys of high-fat diet-induced obese mice. *Am J Physiol Renal Physiol* 2009; 296: F118-F126.
29. Frid A, Sterner GN, Londahl M, Wiklander C, Cato A, Vinge E, Andersson A. Novel assay of metformin levels in patients with type 2 diabetes and varying levels of renal function. *Diabetes Care* 2010; 33: 1291-1293
30. Hayashi T, Hirshman MF, Fujii N, Habinowski SA, WItters LA, Goodyear LJ. Metabolic stress and altered glucose transport activation of AMP-activated protein kinase as a unifying coupling mechanism. *Diabetes* 2000; 49: 527-531
31. Lee MJ, Feliers D, Mariappan MM, Sataranatarajan K, Mahimainathan L, Musi N, Foretz M, Viollet B, Weinberg JM, Choudhury GG, Kasinath BS. A role for AMP-activated protein kinase in diabetes-induced renal hypertrophy. *Am J Physiol Renal Physiol* 2007; 292: 617-627
32. Papandreou I, Cairns RA, Fontana L, Lim AL, Denko NC. HIF-1 mediates adaptation to hypoxia by actively downregulating mitochondrial oxygen consumption. *Cell Metab* 2006; 3; 187-197

33. Biju MP, Akai Y, Shrinmanker N, Haase VH. Protection of HIF-1-deficient primary renal tubular epithelial cells from hypoxia-induced cell death is glucose dependent. *Am J Physiol Renal Physiol* 2005; 289: F1217-F1226
34. Hutchinson DS, Csikasz RI, Yamamoto DL, Shabalina IG, Wikström P, Wilcke M, Bengtsson T. Diphenylene iodonium stimulates glucose uptake in skeletal muscle cells through mitochondrial complex I inhibition and activation of AMP-activated protein kinase. *Cell Signal* 2007; 19: 1610-1620
35. Lambert AJ, Buckingham JA, Boysen HM, Brand MD. Diphenyleneiodonium acutely inhibits reactive oxygen species production by mitochondrial complex I during reverse, but not forward electron transport. *Biochim Biophys Acta* 2008; 1777: 397-403
36. Anedda A, Rial E, Gonzalez-Barroso MM. Metformin induces oxidative stress in white adipocytes and raises uncoupling protein 2 levels. *J Endocrinol* 2008;199, 33-40
37. Ohtomo S, Izuhara Y, Takizawa S, Yamada N, Kakuta T, van Ypersele de Strihou C, Miyata T. Thiazolidinediones provide better renoprotection than insulin in an obese, hypertensive type II diabetic rat model. *Kidney Int* 2007; 72: 1512-1519
38. El-Mir MY, Nogueira V, Fontaine E, Averet N, Rigoulet M, Leverve X. Dimethylbiguanide inhibits cell respiration via indirect effect targeted on the respiratory chain complex I. *J Biol Chem* 2000; 275: 223-228
39. Owen MR, Doran E, Halestrap AP. Evidence that metformin exerts its anti-diabetic effects through inhibition of complex 1 of the mitochondrial respiratory chain. *Biochem J* 2000; 348: 607-614
40. Hawley S, Gadalla AE, Oslen GS, Hardie DG. The antidiabetic drug metformin activates the AMP-activated protein kinase cascade via an adenine nucleotide-independent mechanism. *Diabetes* 2002; 51: 2420-2425
41. Forez M, Hebrard S, Leclerc J, Zarrinpashneh E, Soty M, Mithieux G, Sakamoto K, Andreelli F, Viollet B. Metformin inhibits hepatic gluconeogenesis in mice independently of the LKB1/AMPK pathway via a decrease in hepatic energy state. *J Clin Invest* 2010; 120: 2355-2369
42. Hagen T, Taylor CT, Lam F, Moncada S. Redistribution of intracellular oxygen in hypoxia by nitric oxide: effect on HIF1α. *Science* 2003; 302:1975-1978
43. Fujii N, Jessen N, Goodyear LJ. AMP-activated protein kinase and the regulation of glucose transport. *Am J Physiol Endocrinol Metab* 2006; 291: 867-877

44. Hue L, Beauloye C, Bertrand L, Horman S, Krause U, Marsin AS, Meisse D, Vertommen D, Rider MH. New targets of AMP-activated protein kinase. *Biochem Soc Trans* 2003; 31: 213-215
45. Hochachka PW, Buck LT, Doll CJ, Land SC. Unifying theory of hypoxia tolerance: molecular/metabolic defense and rescue mechanisms for surviving oxygen lack. *Proc Natl Acad Sci USA* 1996; 93: 9493-9498
46. Higgins DF, Biju MP, Akai Y, Wutz A, Johnson RS, Haase VH. Hypoxic induction of Ctgf is directly mediated by Hif-1. *Am J Physiol Renal Physiol* 2004; 287: F1223-F1232
47. Manotham K, Tanaka T, Matsumoto M, Ohse T, Inagi R, Miyata T, Kurokawa K, Fujita T, Ingelfinger JR, Nangaku M. Transdifferentiation of cultured tubular cells induced by hypoxia. *Kidney Int* 2004; 65: 871-880.
48. Tanaka T, Miyata T, Inagi R, Kurokawa K, Adler S, Fujita T, Nangaku M. Hypoxia-induced apoptosis in cultured glomerular endothelial cells: involvement of mitochondrial pathways. *Kidney Int* 2003; 64: 2020-2032
49. Norman JT, Clark IM, Garcia PL. Hypoxia promotes fibrogenesis in human renal fibroblasts. *Kidney Int* 2000; 58: 2351-2366

Table 1. Data collected at 39 week.

	ZDF $^{fa/+}$ (lean) n = 6	ZDF $^{fa/fa}$ (diabetic)		
		untreated n=4	Metformin n=4	Insulin n=6
Body weight, g	496.17 ± 13.48	403 ± 4.97	457 ± 61.52	631 ± 36.14 ^{b,d,f}
Food intake, g/day	13.98 ± 3.11	39.81 ± 2.50 ^{b}	33.63 ± 9.25 ^{b}	22.38 ± 3.79 ^{b,d,f}
Fed glucose, mg/dl	132.17 ± 15.33	573.50 ± 19.50 ^{b}	451.00 ± 116.55 ^{b}	296.33 ± 100.76 ^{b,d,f}
HbA_1c , %	3.43 ± 0.27	10.38 ± 0.59 ^{b}	7.88 ± 1.27 ^{b,d}	5.73 ± 1.15 ^{b,d,f}
Urine volume, ml/day	8.55 ± 2.44	148.73 ± 11.61 ^{b}	85.48 ± 48.77 ^{b,d}	32.92 ± 14.07 ^{d,f}
Urinary albumin, mg/kg/day	6.85 ± 3.48	349. 44 ± 92.55 ^{b}	203.80 ± 121.32 ^{b,c}	108.51 ± 45.69 ^{b,d,e}
HIF- α immunoreactivity	0.0 ± 0.0	2.0 ± 1.16^{b}	0.5 ± 0.58 ^{c}	1.17 ± 0.41 ^{a}
Tubular injury	0.0 ± 0.0	3.0 ± 0.0 ^{b}	1.75 ± 0.96 ^{b,d}	2.5 ± 0.55 ^{b}

Values are means ±SD. ^{a}P<0.05, ^{b}P<0.01 *vs* lean rats; ^{c}P <0.05, ^{d}P<0.01 *vs* untreated diabetic rats; ^{e}P <0.05, ^{f}P<0.01 *vs* metformin-treated rats;

FIGURE LEGENDS

FIG. 1. ***A:*** Metformin inhibits hypoxia-induced HIF-1α protein expression. HRPTECs were treated with 1 mM metformin and 1 mM AICAR under normoxic and hypoxic conditions overnight. Whole cell protein extracted from HRPTECs was analyzed by Western blot analysis. Although AICAR stimulated the phosphorylation of AMP-activated protein kinase (AMPK) and ACC and inhibited the phosphorylation of mTOR much like metformin, AICAR failed to suppress hypoxia-induced HIF-1α expression. ***B:*** Metformin inhibits hypoxia-induced HIF-1α protein expression. HRPTECs were treated with or without 1 mM metformin under normoxic (21% O_2) and hypoxic (1% O_2) conditions overnight. Whole cell proteins were extracted and analyzed for HIF-1α expression by Western blot. Metformin inhibited hypoxia-induced HIF-1α expression. Densitometric analysis showed that hypoxia significantly induced HIF-1α protein expression compared to that in control in normoxia, and that metformin decreased hypoxia-induced HIF-1α expression to approximately 15.4 % of that of control in hypoxia. $^{\#\#}P<0.01$ versus control under normoxic conditions, $^{**}P<0.01$ versus control under hypoxic conditions. ***C*****:** Metformin inhibits hypoxia-induced HIF-1α accumulation. HRPTECs were incubated in serum-free DMEM with 0.01-1

mM metformin under hypoxic conditions. After 4 hours, cells were harvested for Western blot analysis. ***D*:** The inhibitory effect of metformin on hypoxia-induced HIF-1α expression was significantly detectable at 0.01 mM. **P<0.01 versus control under hypoxic conditions, $^{\$\$}$P<0.01 versus 0.01 mM metformin-treated cells under hypoxic conditions. ***E-H:*** Quantitative real-time reverse transcription-PCR analysis of HIF-1α and HIF-1 target genes. HRPTECs were treated with or without 10 mM metformin under normoxic and hypoxic conditions overnight. Then, total RNA was extracted from HRPTECs and was applied for quantitative RT-PCR. The relative amounts of PAI-1, VEGF and Glut-1 mRNA were normalized by 18S and expressed as an arbitrary unit in which the control group value equaled 1. Hypoxia significantly induced PAI-1, VEGF, and Glut-1 mRNA expression in HRPTECs, and 10 mM metformin inhibited the induction of this mRNA expression by hypoxia. Data represent means ± SD (n=3). $^{\#\#}$P<0.01 versus control under normoxic conditions, *P<0.05, **P<0.01 versus control under hypoxic conditions.

FIG. 2. Metformin inhibited hypoxia-induced HIF-1α protein expression independent of AMPK. ***A-D*:** HRPTECs were transiently transfected with control, AMPK-α1 or -α2-specific siRNAs (25 nM final concentration). Forty-eight hours after transfection,

cells were serum-starved for an additional 24 h and subsequently treated as indicated under normoxic or hypoxic conditions for 4h, and cells were lysed and subjected to immunoblotting with specific antibodies indicated. Lowering AMPK-α1 (***A, B***) or AMPK-α2 (***C, D)*** protein expression with specific siRNA failed to restore the inhibitory effects of metformin on hypoxia-induced HIF-1α protein expression. $^{\#}P<0.05$, $^{\#\#}P<0.01$ versus non-treated cells, $^{*}P<0.05$, $^{**}P<0.01$ versus control siRNA-transfected cells, $^{\$}P<0.05$, $^{\$\$}P<0.01$ versus AMPK-α1 or -α2 siRNA-transfected cells under hypoxic conditions. ***E*.** The proteasomal inhibitor MG-132 (10 μM) abolished the inhibitory effect of 10 mM metformin on HIF-1α accumulation under hypoxic conditions for 4 hr. Whereas, an AMPK inhibitor, compound C (20 μM) failed to antagonize the inhibitory effect of metformin on HIF-1α protein expression.

FIG. 3. Effects of high glucose on the inhibitory effects of metformin on hypoxia-induced HIF-1α expression. ***A:*** HRPTECs were treated with high $_{D}$-glucose (25 mM) and 1mM metformin under normoxic and hypoxic conditions overnight. Whole cell proteins extracted from HRPTECs were then analyzed by Western blot. Although high glucose attenuated the stimulatory effects of metformin on the expression of p-AMPK and p-ACC and the inhibitory effects of metformin on the

expression of p-mTOR, high glucose did not blunt the inhibitory effect of metformin on HIF-1α expression. $_{L}$-glucose (25 mM) as an osmolarity control also did not alter the effects of metformin. ***B:*** Densitometric analysis showed that high glucose did not affect HIF-1α protein expression in hypoxia, and that metformin still decreased hypoxia-induced HIF-1α expression to more than 80 % of that of control in hypoxia independent of glucose concentrations. $^{**}P<0.01$.

FIG. 4. ***A:*** Effects of inhibitors of mitochondrial pyruvate transport, mTOR and mitochondrial respiratory complexes I and III, on the expression of hypoxia-induced HIF-1α. HRPTECs were treated with inhibitors of mitochondrial pyruvate transport (CHC, 0.1 mM), mTOR (rapamycin, 100 nM) and with 1 mM metformin under normoxic and hypoxic conditions for 4 h. These inhibitors failed to decrease hypoxia-induced HIF-1α accumulation. ***B:*** The inhibitors for mitochondrial respiratory complexes I and III inhibits hypoxia-induced HIF-1α accumulation. The cells were treated with mitochondrial respiratory complex I (rotenone, 0.25 μM, 25 μM), mitochondrial respiratory complex III (antimycin A, 10 ng/ml, 1 μg/ml) and with 1 mM metformin under hypoxic conditions for 4 h. The inhibition of mitochondrial respiration suppressed HIF-1α protein expression, accompanied with increased expressions of

p-AMPK and p-ACC, and decreased p-mTOR expression. ***C, D*:** Metformin suppressed mitochondrial respiratory functions of HRPTECs in normoxia and hypoxia in medium containing 5.5 mM (low) (***C***) or 25 mM (high) (***D***) glucose. Cells treated with indicated reagents were incubated in normoxia (21% O_2) or hypoxia (1% O_2) for 4 hr, and then resuspended in normoxic medium. Oxygen consumption was measured in a sealed chamber using a Clark-type electrode. Hypoxia decreased oxygen consumption down to 76.5 % of the control in normoxia in low glucose ($^{**}p<0.01$) (***C***). This response to hypoxia was blunted by 25 mM glucose (***D***). Metformin significantly inhibited oxygen consumption to less that 50 % of controls, independent of the oxygen conditions or the glucose milieu ($^{*}p<0.05$, $^{**}p<0.01$). Data are expressed as mean ± SD (n=3). ***E, F:*** Cell ATP during metformin or AICAR treatment under normoxia and hypoxia in medium containing 5.5 mM (low) (***E***) or 25 mM (high) (***F***) glucose. HRPTECs were incubated with indicated reagents in normoxia or hypoxia for 4 hr. At the end of incubation, cells were extracted with perchloric acid for the measurement of ATP as described in *Methods*. Protein was determined in parallel dishes. Cell ATP was normalized with protein. Data are expressed as mean ± SD (n=3). The results show that cell ATP in medium containing low glucose was trend to decrease during metformin treatment under either normoxic or hypoxic conditions in contrast to the enhancement

of ATP production by the treatment of AICAR ($^{*}p<0.05$, $^{**}p<0.01$) (***E***). In contrast, 25 mM glucose attenuated ATP levels and the inhibitory effects of metformin on ATP levels in normoxia and hypoxia (***F***).

FIG. 5. ***A:*** An antioxidant NAC had no effect on hypoxia-induced HIF-1α protein expression. HRPTECs were treated with 1 mM metformin, NADPH oxidase inhibitors (DPI, 10 μM), the antioxidant (NAC, 5 mM), metformin under normoxic and hypoxic conditions for 4 h. NAC did not inhibit hypoxia-induced HIF-1α expression, indicating that mitochondrial ROS production was not involved in HIF-1α stabilization. ***B*****:** NADPH contents in HRPTECs. Both metformin and AICAR restored hypoxia-decreased NADPH contents. Data are expressed as mean ± SD (n=3). *, $p<0.05$. ***C:*** Effects of metformin on reactive oxygen species (ROS) production in HRPTECs. Intracellular ROS were measured with DHE, which produces a red fluorescence in typically nuclear localization when oxidized to ethidium bromide by O_2^-. HRPTECs were treated with 1 mM metformin or 1 mM AICAR overnight under normoxic or hypoxic conditions in medium containing 5.5 mM (low) or 25 mM (high) glucose. In medium containing low glucose, hypoxia decreased DHE staining and metformin increased DHE staining in contrast to AICAR. High glucose enhanced DHE

staining in normoxia and hypoxia. Metformin suppressed the high glucose-induced ROS production in normoxia, and did not increase DHE staining even under hypoxic conditions and in a high-glucose milieu. (Original magnification, x200). ***D:*** Detection of hypoxic state in HRPTECs. The cells were grown on the cover slides until subconfluence and then treated overnight as indicated. HRPTECs under normoxic conditions showed no staining for HIF-1α. Hypoxia induced nuclear expression of HIF-1α in HRPTECs, and 1 mM metformin inhibited hypoxia-induced HIF-1α nuclear staining. 1 mM AICAR did not affect the expression of HIF-1α in HRPTECs under hypoxic conditions. (*upper panel*). Hypoxia of HRPTECs was detected by the use of pimonidazole hydrochloride (*lower panel*). Metformin, not AICAR, increased cellular oxygen tension in HRPTECs under hypoxic conditions. Nuclei were stained with DAPI. Original magnification, x 800.

FIG. 6. *A*: Immunohistochemistry for the hypoxia marker pimonidazole. Rats were studies at eight weeks of treatment by metformin or by insulin. Scar bars represent 300 μm (*left row*), 30 μm (right row). ***B:*** Intensity of pimonidazole staining was increased in tubular cells of the kidney cortex of ZDF, which was significantly attenuated by metformin treatment, not by insulin. $^{**}p<0.01$. ***C*:** Immunohistochemical analysis of HIF-1α expressions and light micrographs of sections from kidneys stained with the

periodic acid-Schiff (PAS) reagent in Zucker lean control rats (**ZL**) (***a-e***), non-treated ZDF rats (**ZDF**) (***f-j***) and metformin-treated ZDF rats (**ZDF+M**) (***k-o***), and insulin-treated ZDF rats (**ZDF+I**) (***p-t***). In the lean rats (***a-c***) and metformin-treated ZDF rats (***k-m***), HIF-1α positive cells were renal tubular cells in the inner medulla, with few positive cells in the outer medulla and the cortex. In contrast, a marked increase tubular staining for HIF-1α was observed in the outer medulla and cortex of ZDF rats (***f, h***). Lean control rats (ZL) showed no tubular and glomerular injury in kidneys (***d, e***). Notably, severe sclerosed glomeruli and damaged tubules, which present cellular debris, tubular cast formations, interstitial nephritis are observed in sections from ZDF rats (***i, j***). Metformin, but not insulin (***s, t***), ameliorated the tubular injury in the outer medulla and cortex of ZDF rats (***n, o***). Asterisks show the glomeruli. Scar bars represent 300 μm at low power field, 30 μm at high power field.

FIG. 7. Metformin inhibits hypoxia-induced HIF-1α protein expression through the inhibition of mitochondrial respiration. Metformin inhibits oxygen consumption and ATP production by inhibiting mitochondrial complex I. Subsequently, intracellular oxygen redistribution supplies oxygen for prolyl hydroxylase which promotes the degradation of HIF-1α in the proteasome. ATP depletion caused by mitochondrial

inhibition activates AMPK, which is a downstream signaling pathway of mitochondrial respiratory chain complex. Therefore, AICAR activates AMPK pathway, but fails to inhibit hypoxia-induced HIF-1α accumulation.

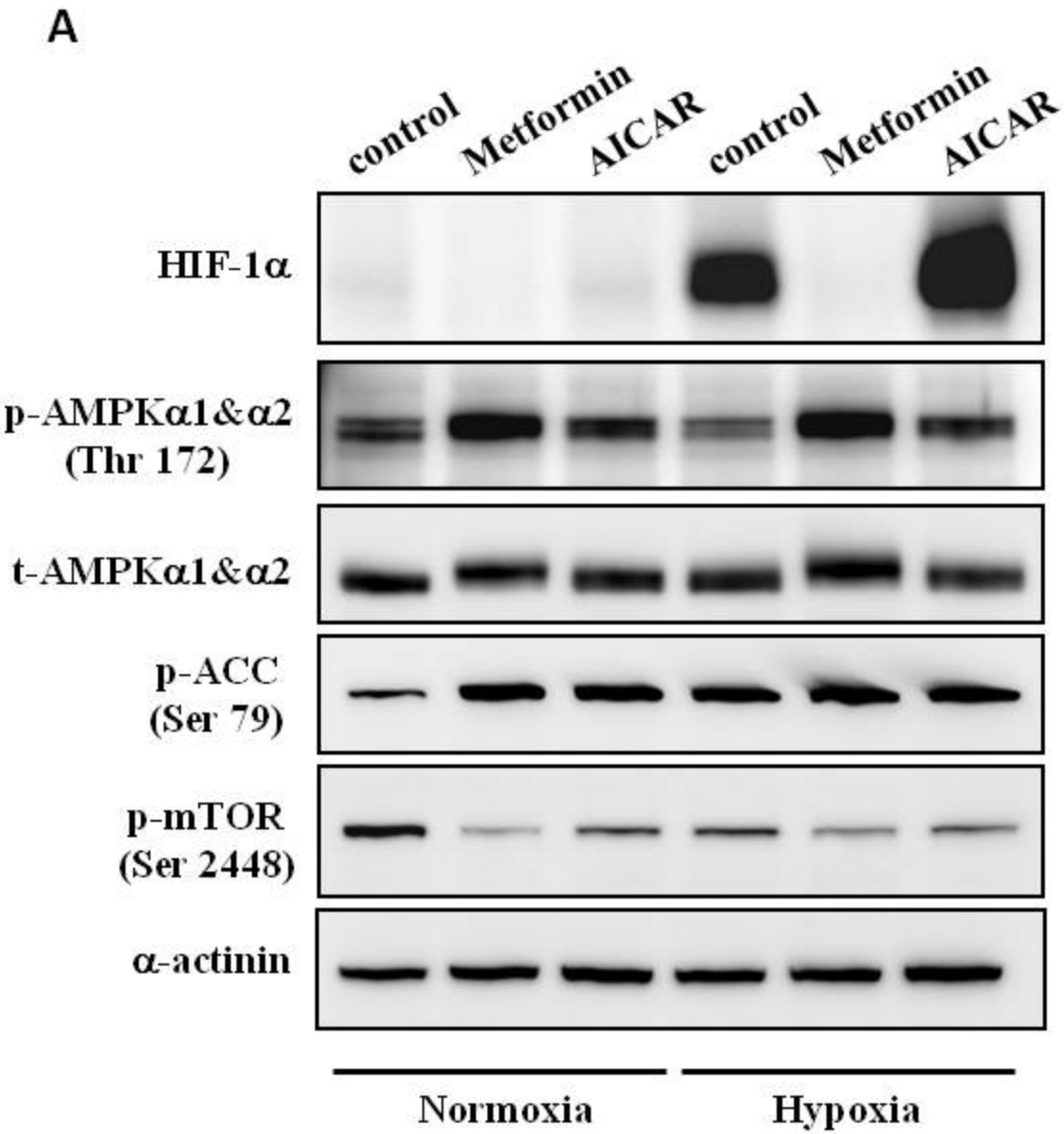
A
control
Metformin
AICAR
control
Metformin
AICAR
HIF-1α
p-AMPKα1&α2
(Thr 172)
t-AMPKα1&α2
p-ACC
(Ser 79)
p-mTOR
(Ser 2448)
α-actinin
Normoxia
Hypoxia

Figure 1.

B

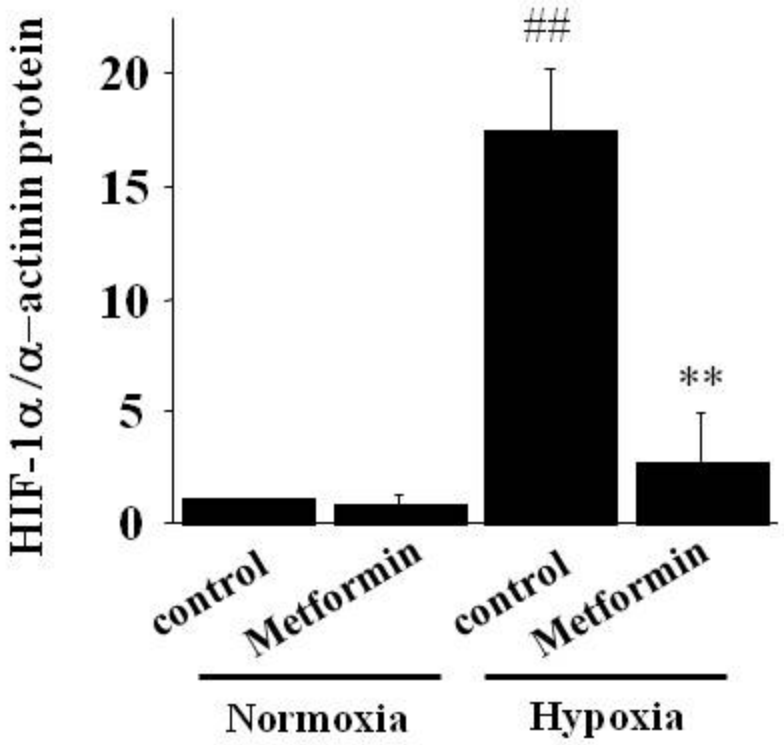
HIF-1α /α–actinin protein
20
15
10
5
0
##
**
control
Metformin
control
Metformin
Normoxia
Hypoxia

Figure 1.

C

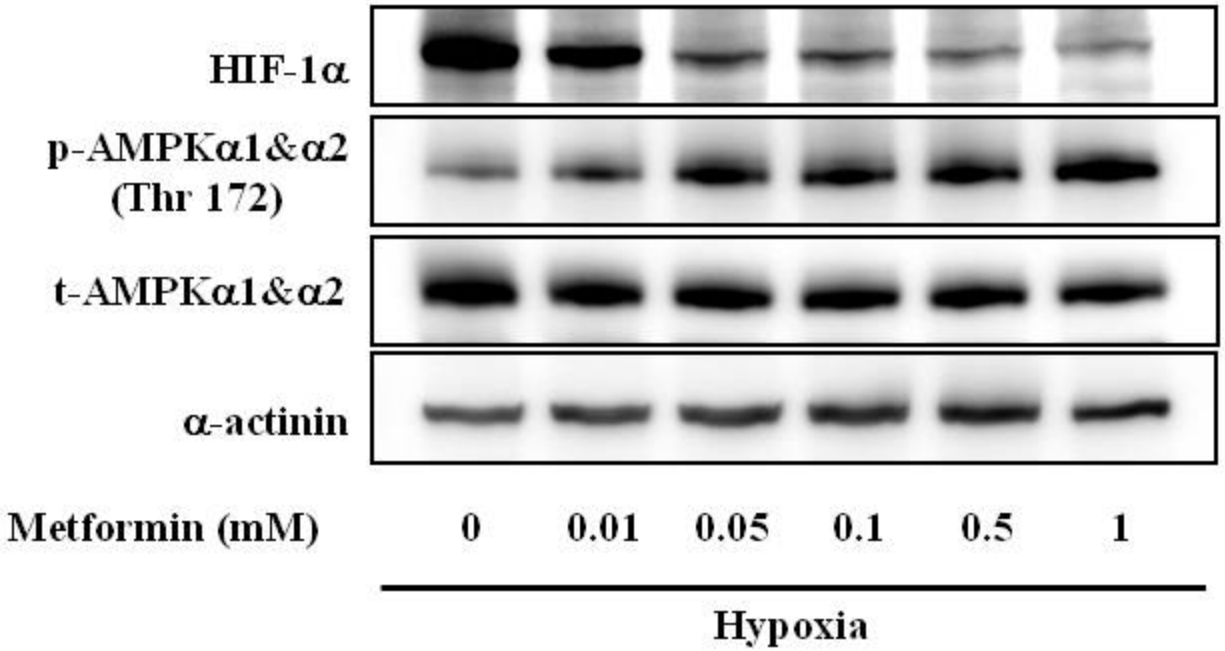
HIF-1α
p-AMPKα1&α2
(Thr 172)
t-AMPKα1&α2
α-actinin
Metformin (mM)
0
0.01
0.05
0.1
0.5
1
Hypoxia

Figure 1.

D

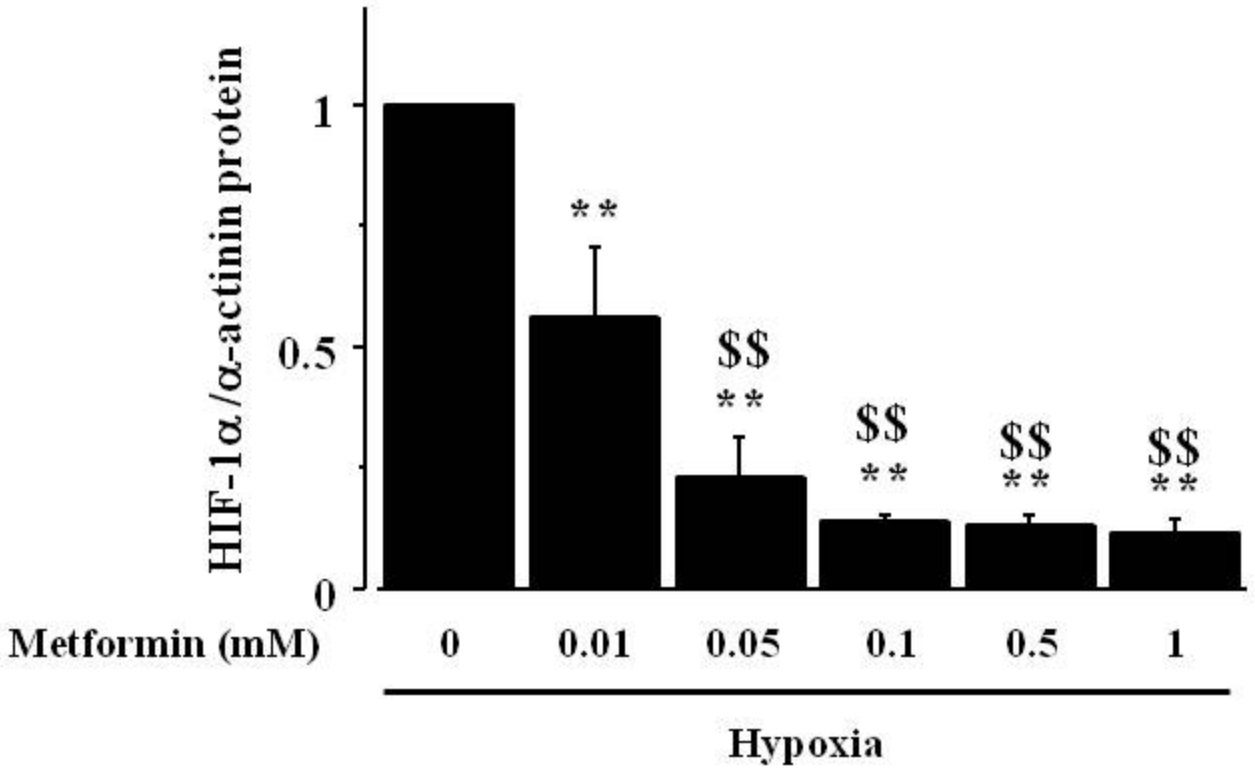
HIF-1α /α-actinin protein
1
0.5
0
**
$$
**
$$
**
$$
**
$$
**
Metformin (mM)
0
0.01
0.05
0.1
0.5
1
Hypoxia

Figure 1.

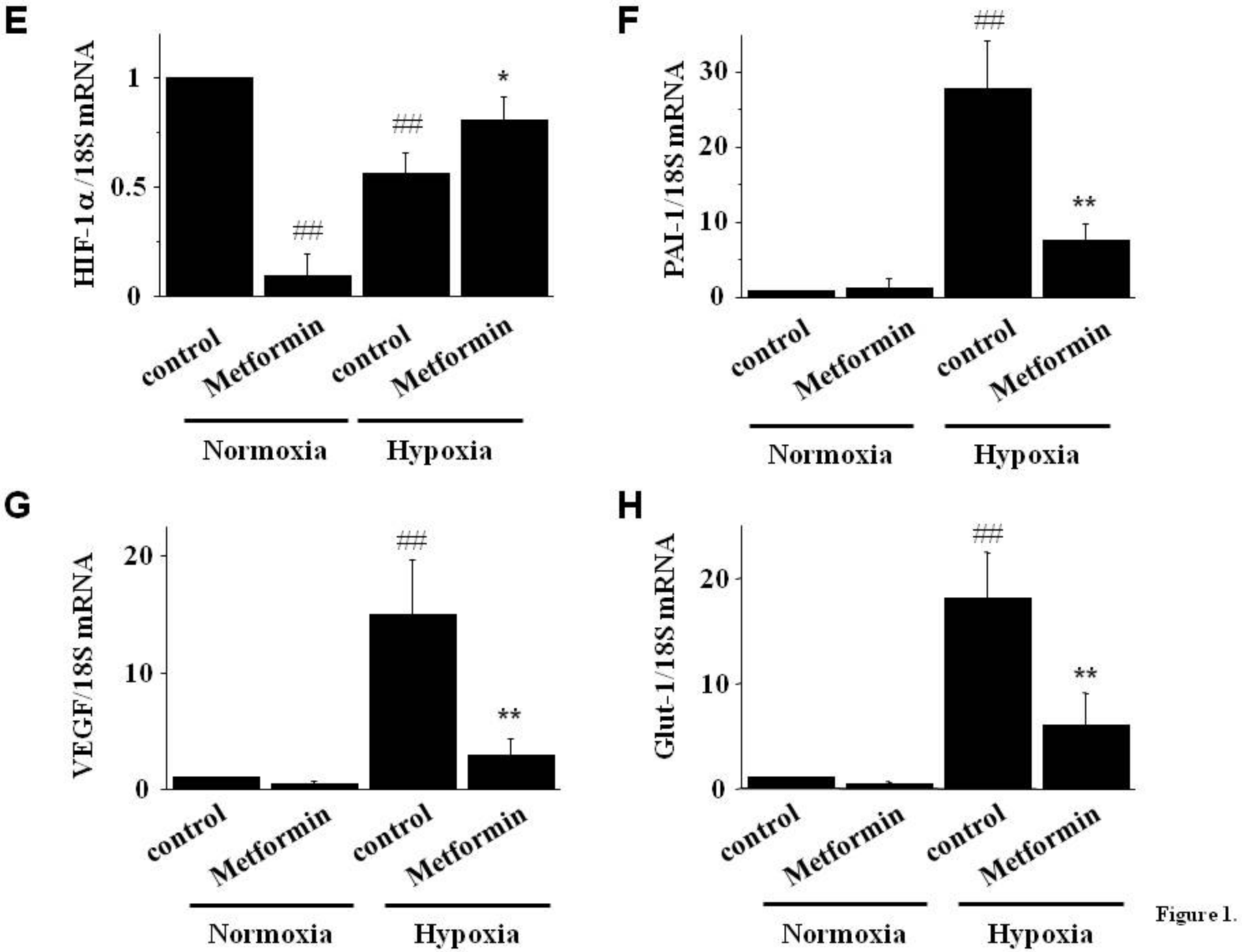
E
HIF-1α/18S mRNA
1
0.5
0
##
##
*
control
Metformin
control
Metformin
Normoxia
Hypoxia
F
PAI-1/18S mRNA
30
20
10
0
##
**
control
Metformin
control
Metformin
Normoxia
Hypoxia
G
VEGF/18S mRNA
20
10
0
##
**
control
Metformin
control
Metformin
Normoxia
Hypoxia
H
Glut-1/18S mRNA
20
10
0
##
**
control
Metformin
control
Metformin
Normoxia
Hypoxia

Figure 1.

A

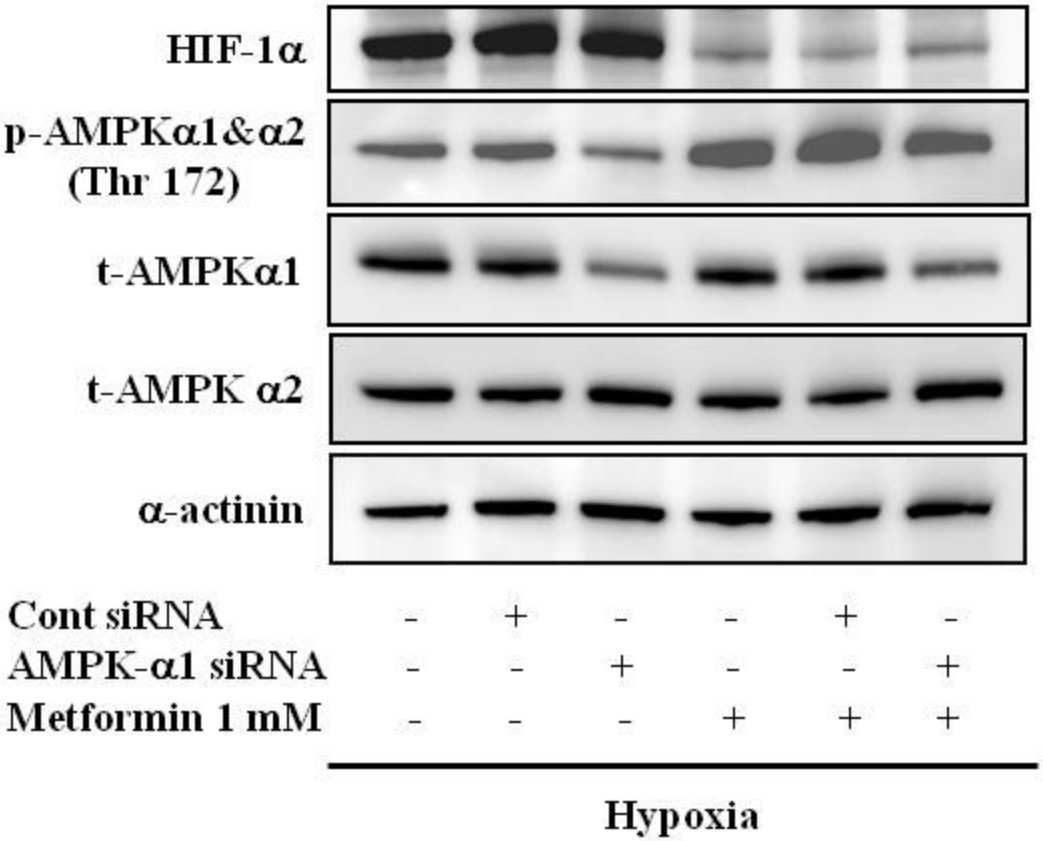
HIF-1α
p-AMPKα1&α2
(Thr 172)
t-AMPKα1
t-AMPK α2
α-actinin
Cont siRNA - + - - + -
AMPK-α1 siRNA - - + - - +
Metformin 1 mM - - - + + +
Hypoxia

Figure 2.

B

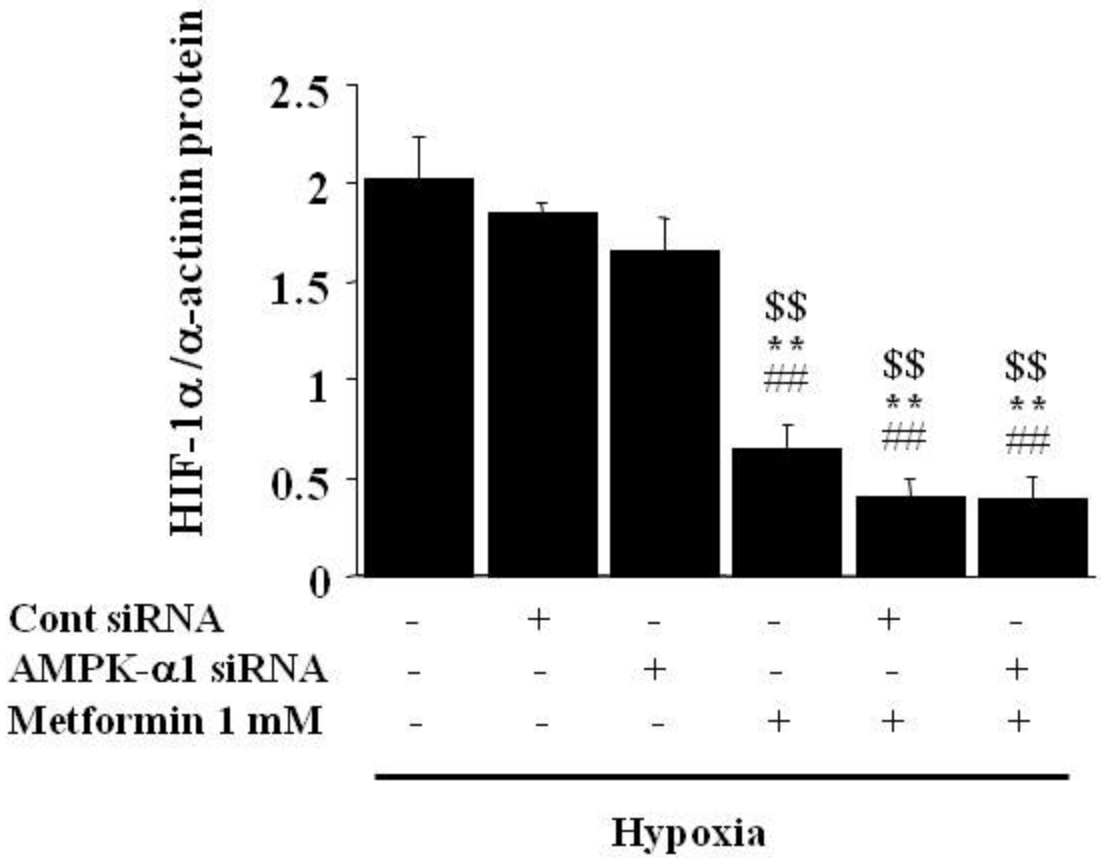
HIF-1α /α-actinin protein
2.5
2
1.5
1
0.5
0
$$
**
##
$$
**
##
$$
**
##
Cont siRNA - + - - + -
AMPK-α1 siRNA - - + - - +
Metformin 1 mM - - - + + +
Hypoxia

Figure 2.

C

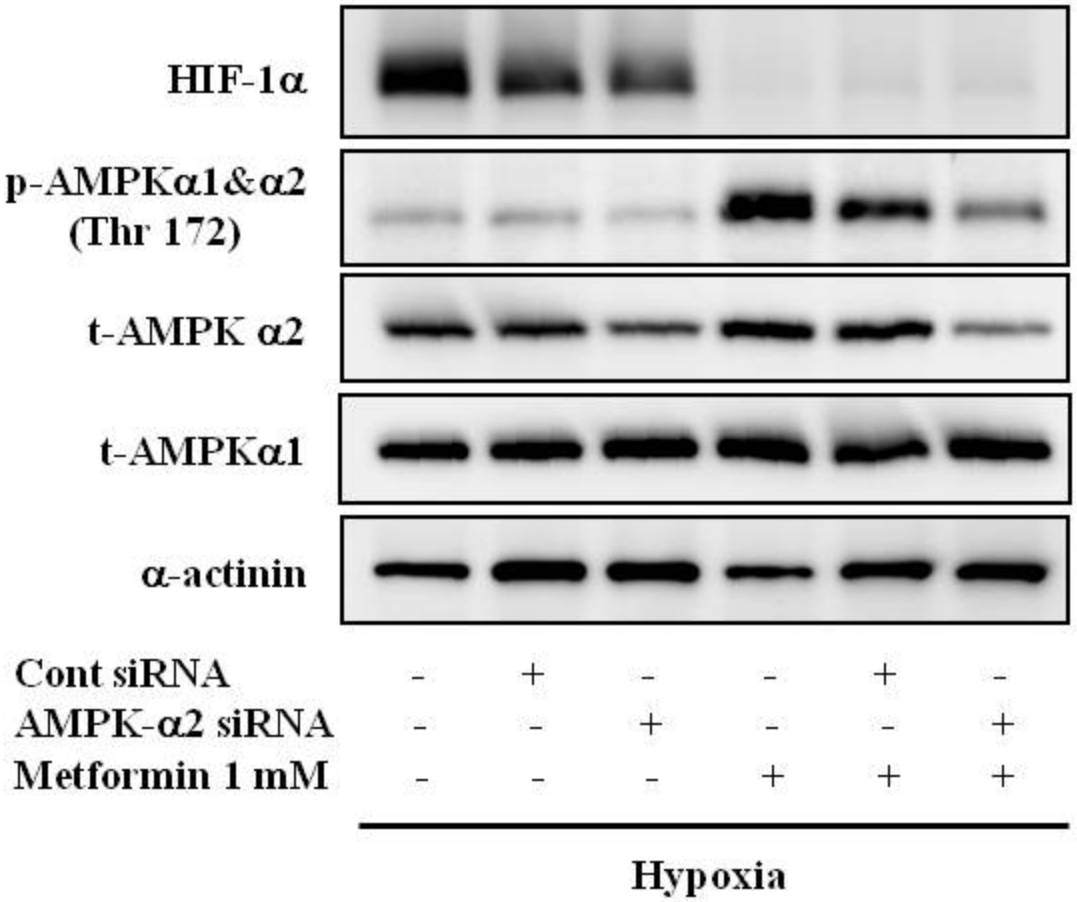
HIF-1α
p-AMPKα1&α2
(Thr 172)
t-AMPK α2
t-AMPKα1
α-actinin
Cont siRNA - + - - + -
AMPK-α2 siRNA - - + - - +
Metformin 1 mM - - - + + +
Hypoxia

Figure 2.

D

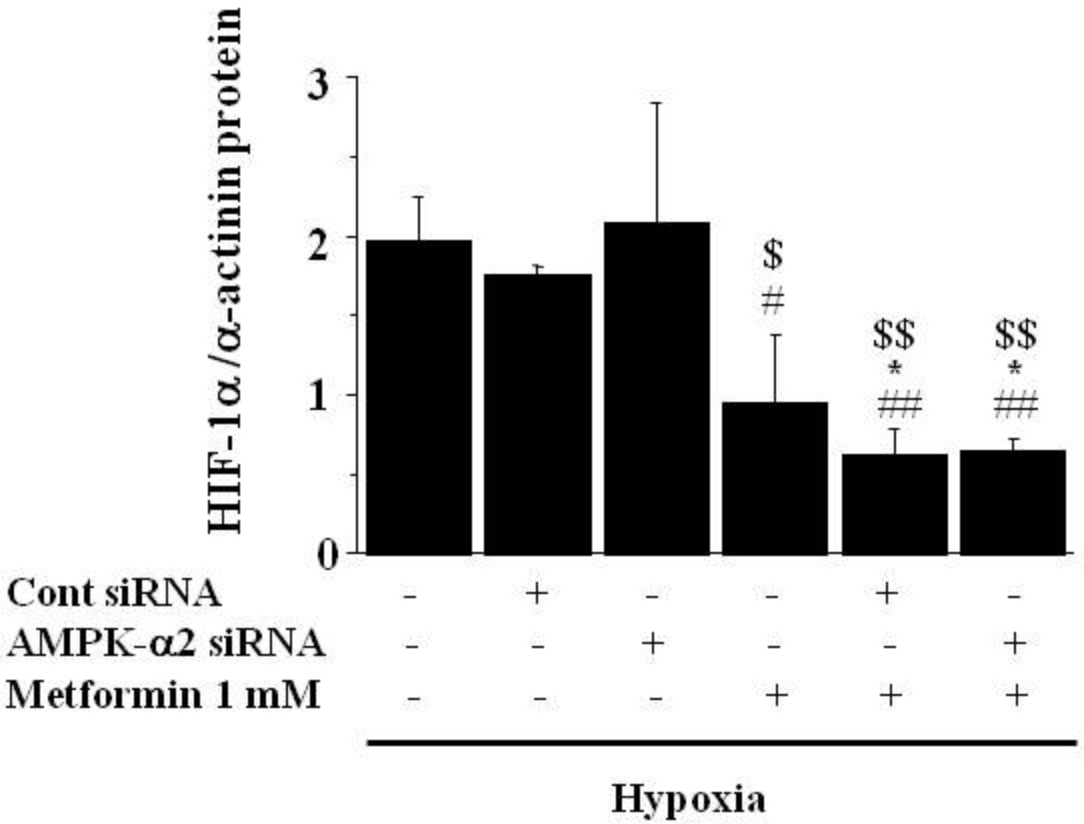
HIF-1α /α-actinin protein
3
2
1
0
$
#
$$
*
##
$$
*
##
Cont siRNA - + - - + -
AMPK-α2 siRNA - - + - - +
Metformin 1 mM - - - + + +
Hypoxia

Figure 2.

E

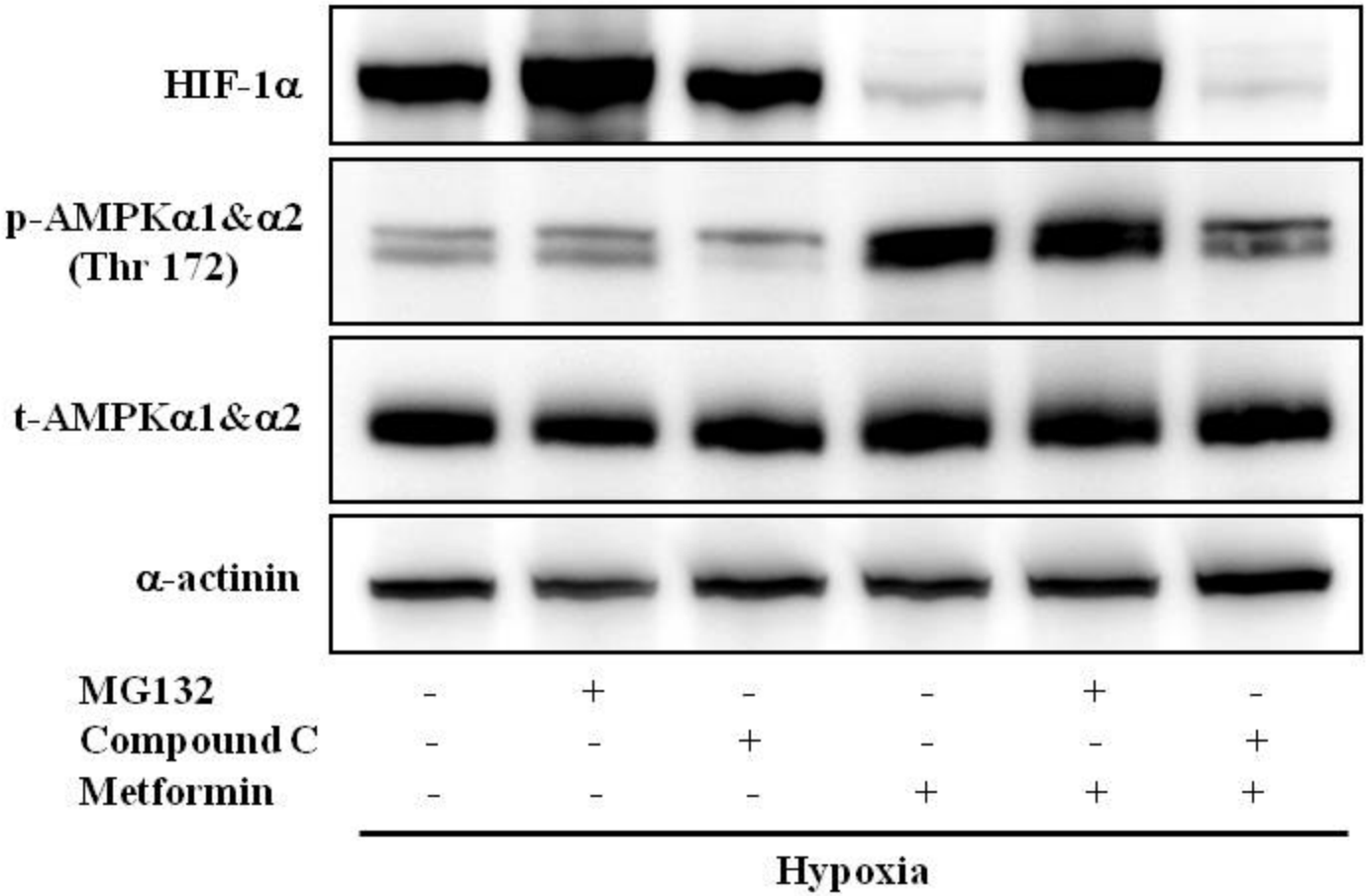
HIF-1α
p-AMPKα1&α2
(Thr 172)
t-AMPKα1&α2
α-actinin
MG132 - + - - + -
Compound C - - + - - +
Metformin - - - + + +
Hypoxia

Figure 2.

A

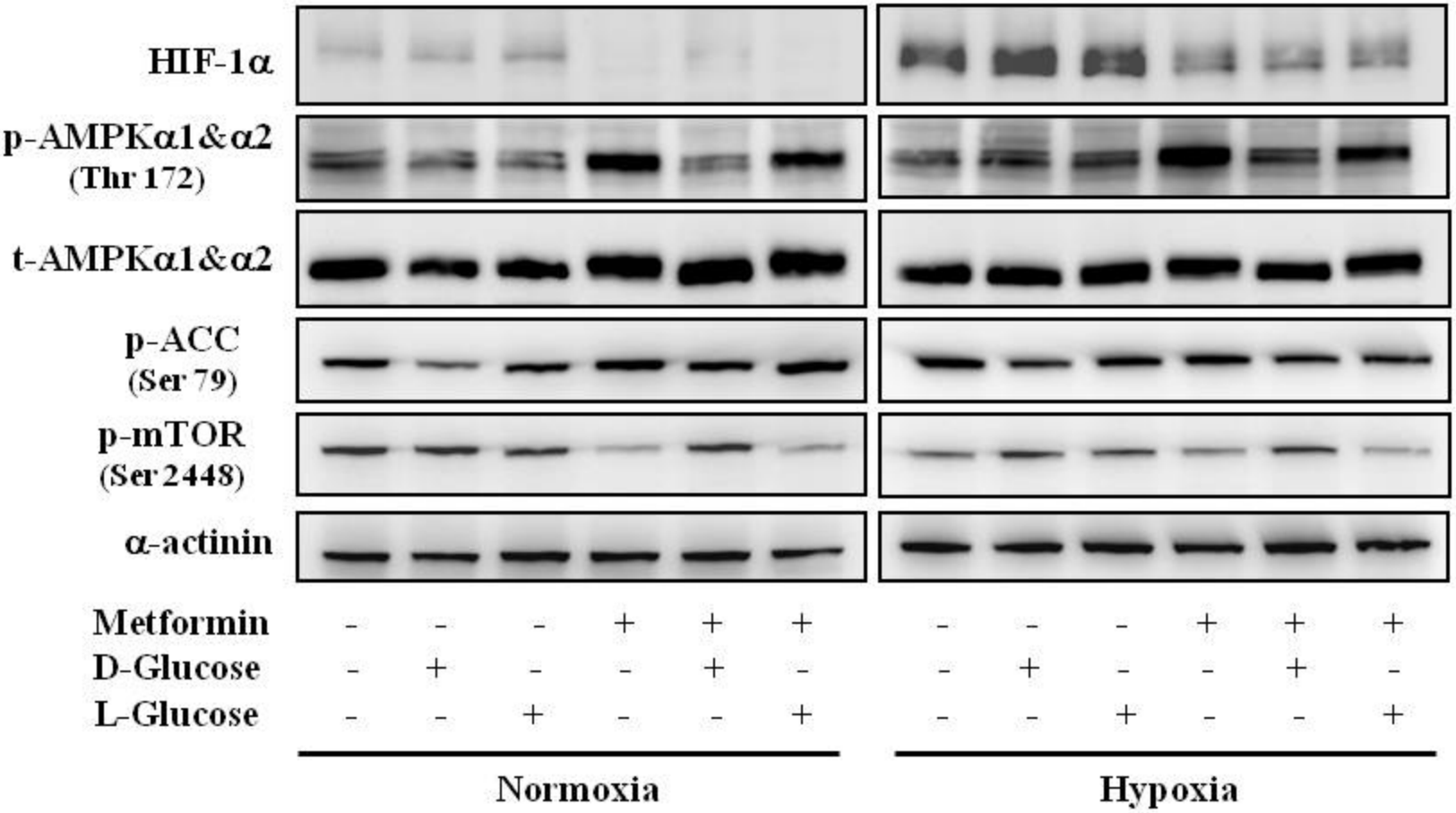
HIF-1α
p-AMPKα1&α2
(Thr 172)
t-AMPKα1&α2
p-ACC
(Ser 79)
p-mTOR
(Ser 2448)
α-actinin
Metformin - - - + + + - - - + + +
D-Glucose - + - - + - - + - - + -
L-Glucose - - + - - + - - + - - +
Normoxia
Hypoxia

Figure 3.

B

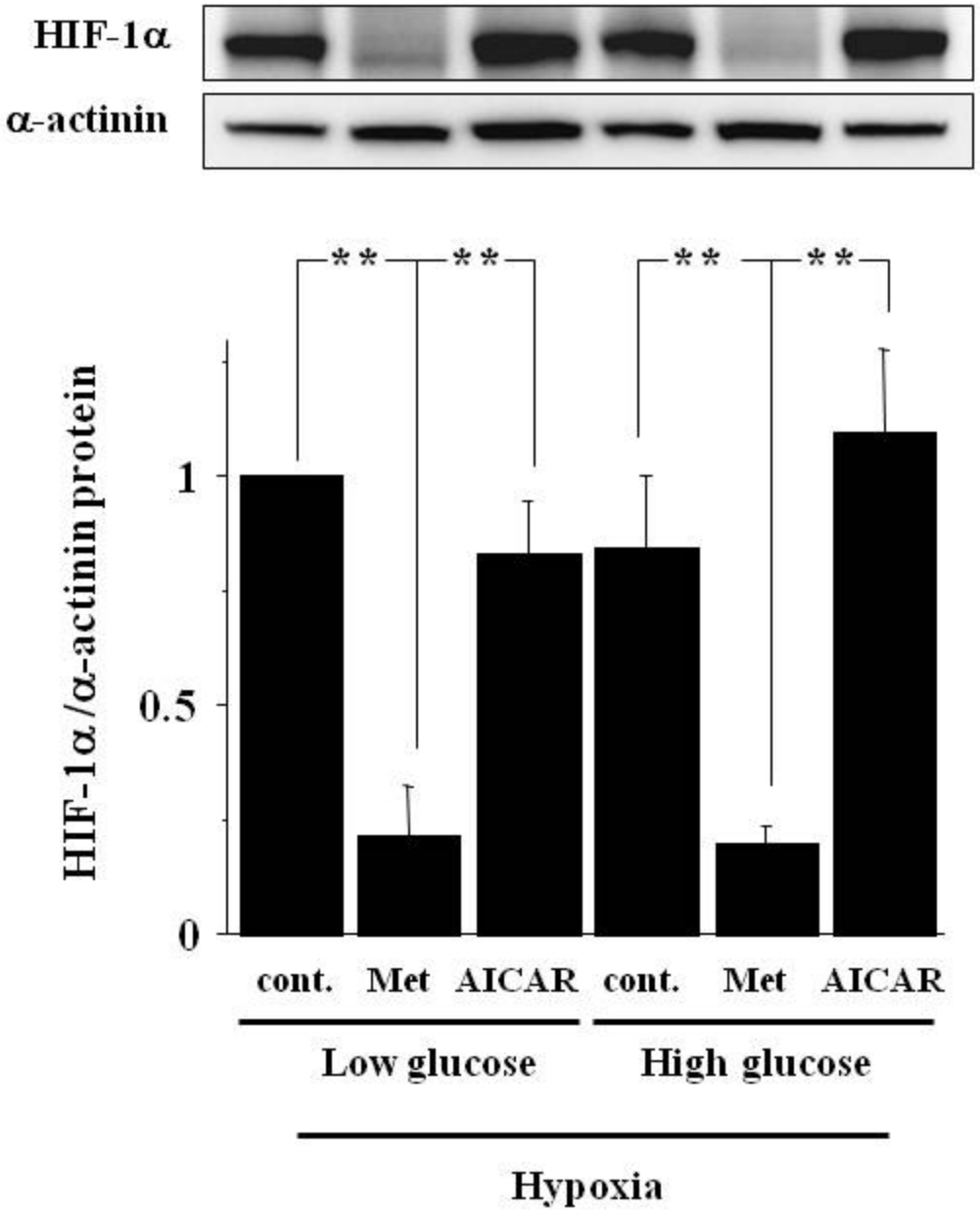
HIF-1α
α-actinin
**
**
**
**
HIF-1α /α-actinin protein
1
0.5
0
cont.
Met
AICAR
cont.
Met
AICAR
Low glucose
High glucose
Hypoxia

Figure 3.

A

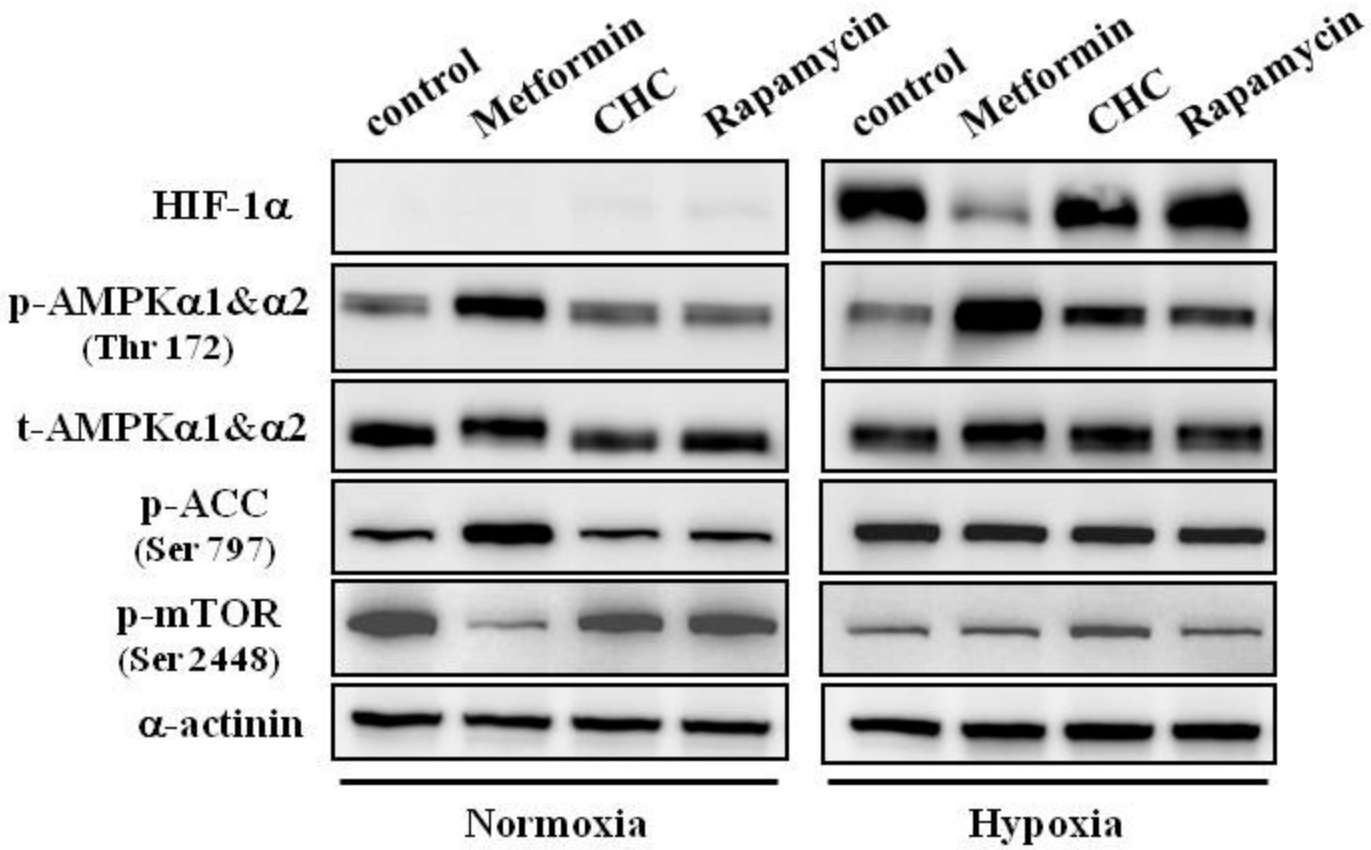
control
Metformin
CHC
Rapamycin
control
Metformin
CHC
Rapamycin
HIF-1α
p-AMPKα1&α2
(Thr 172)
t-AMPKα1&α2
p-ACC
(Ser 797)
p-mTOR
(Ser 2448)
α-actinin
Normoxia
Hypoxia

Figure 4.

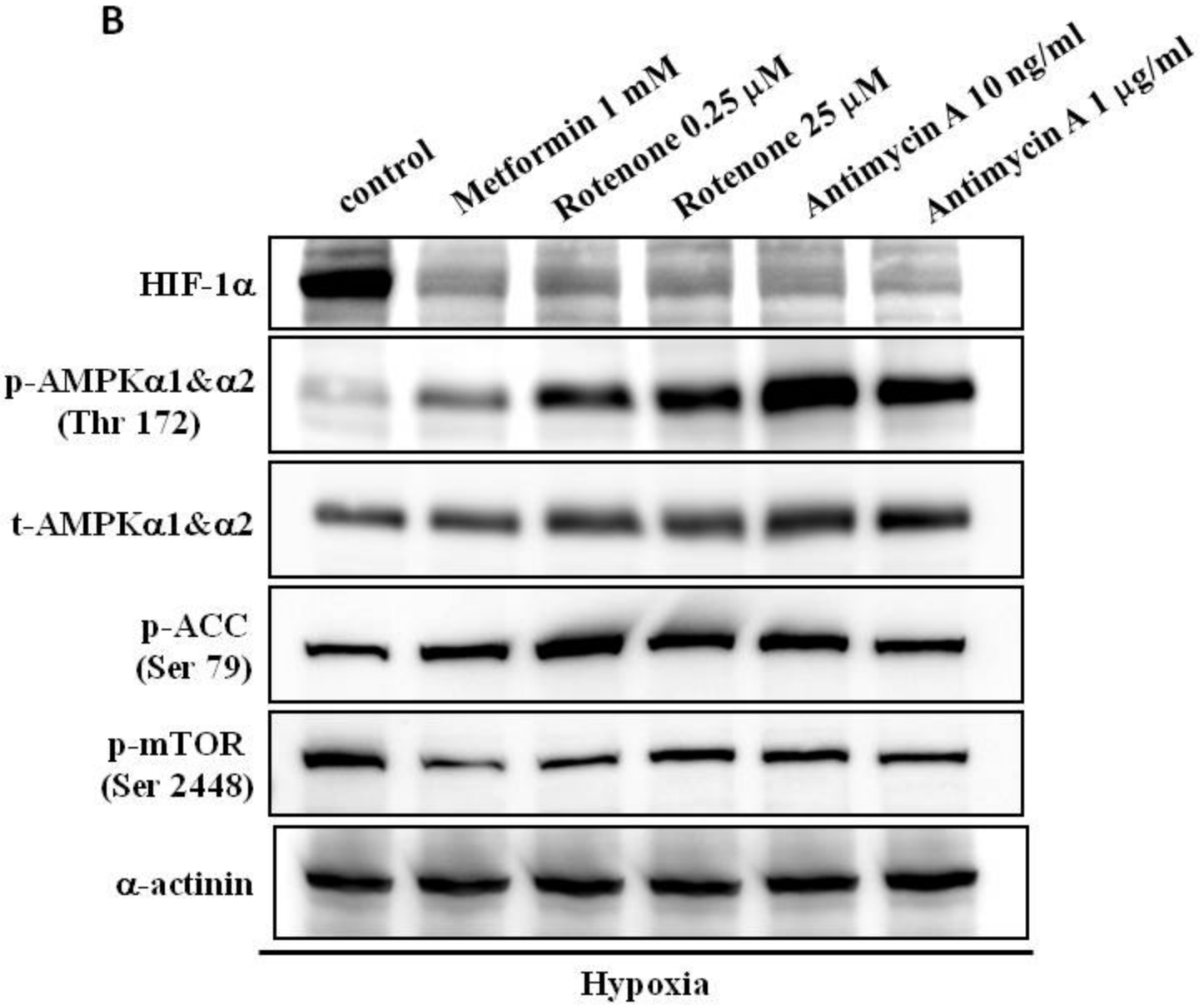
B
control
Metformin 1 mM
Rotenone 0.25 μM
Rotenone 25 μM
Antimycin A 10 ng/ml
Antimycin A 1 μg/ml
HIF-1α
p-AMPKα1&α2
(Thr 172)
t-AMPKα1&α2
p-ACC
(Ser 79)
p-mTOR
(Ser 2448)
α-actinin
Hypoxia

Figure 4.

C

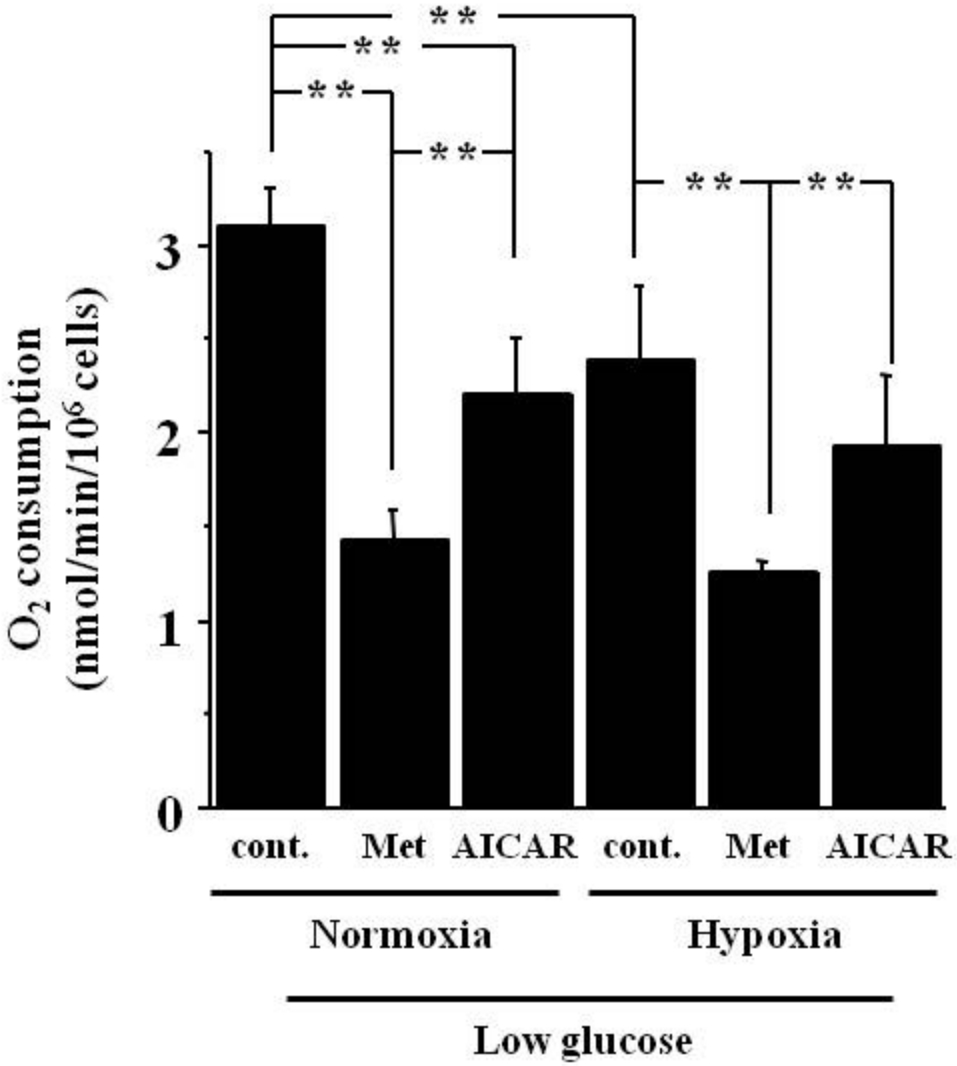
**
**
**
**
**
**
O2 consumption
(nmol/min/10^6 cells)
3
2
1
0
cont.
Met
AICAR
cont.
Met
AICAR
Normoxia
Hypoxia
Low glucose

Figure 4.

D

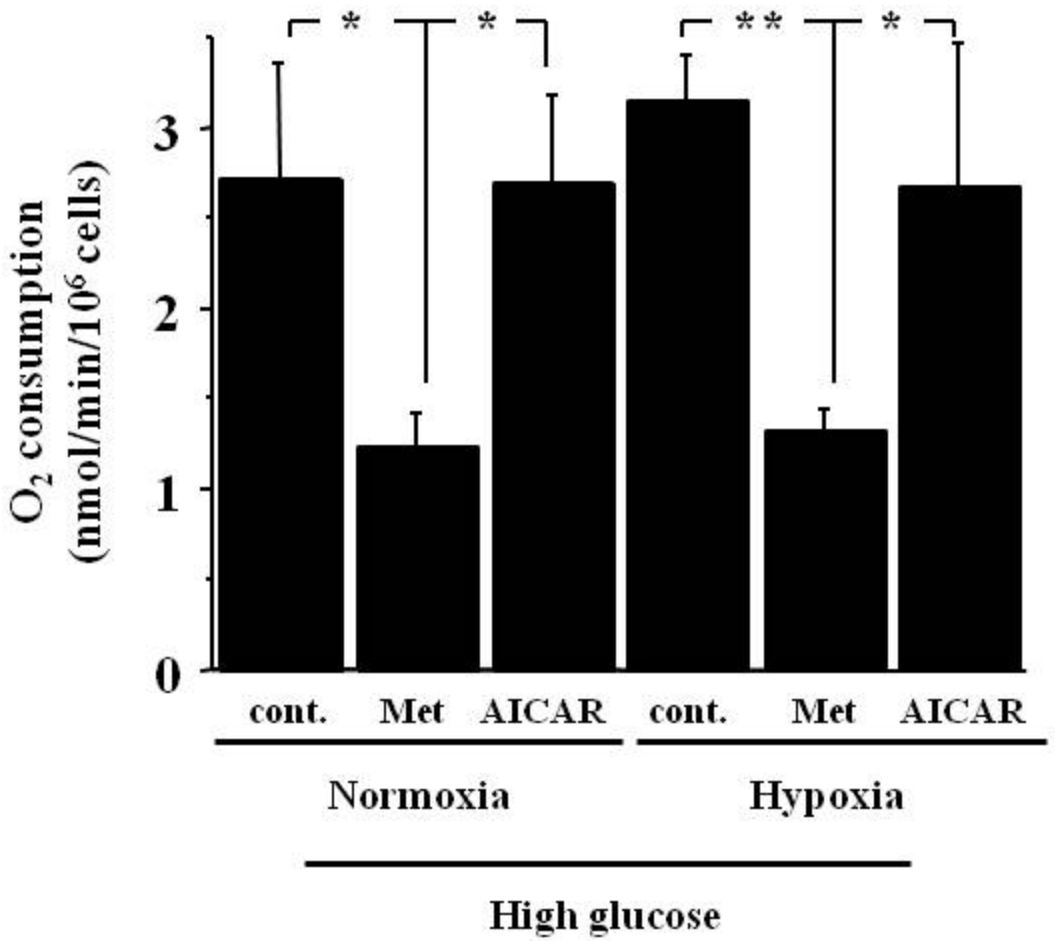
*
*
**
*
3
2
1
0
O_2 consumption
(nmol/min/10^6 cells)
cont.
Met
AICAR
cont.
Met
AICAR
Normoxia
Hypoxia
High glucose

Figure 4.

E

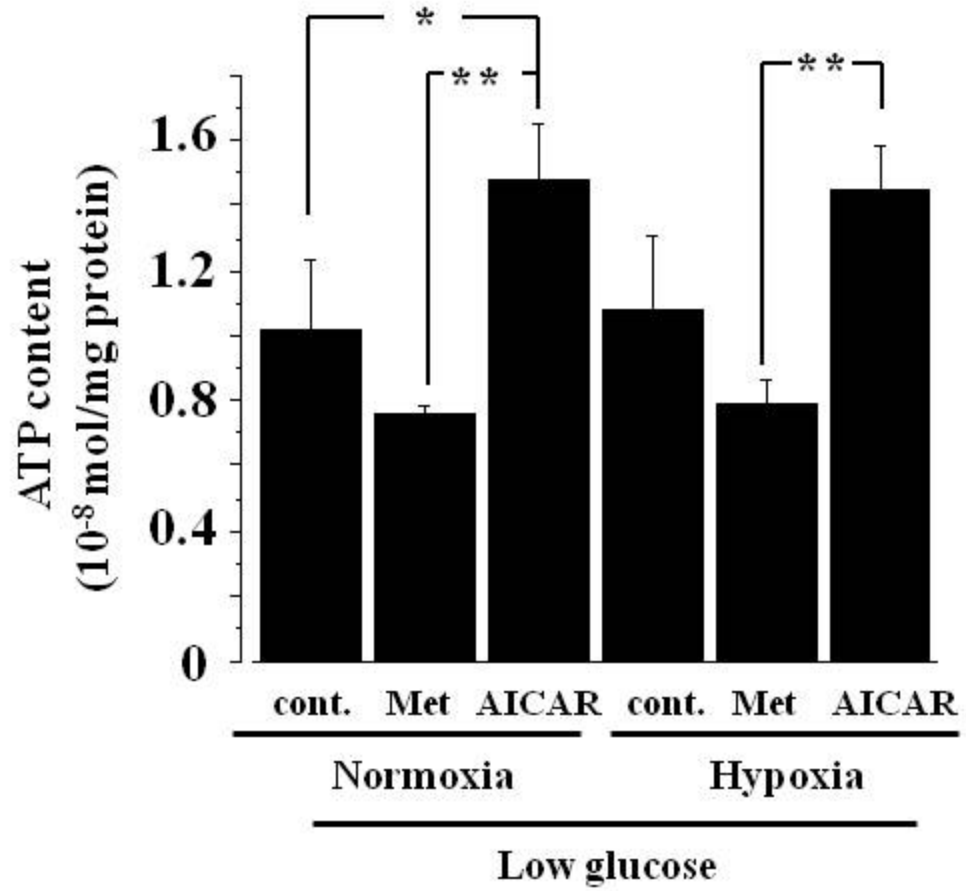
*
**
**
1.6
1.2
0.8
0.4
0
ATP content
(10-8 mol/mg protein)
cont.
Met
AICAR
cont.
Met
AICAR
Normoxia
Hypoxia
Low glucose

Figure 4.

F

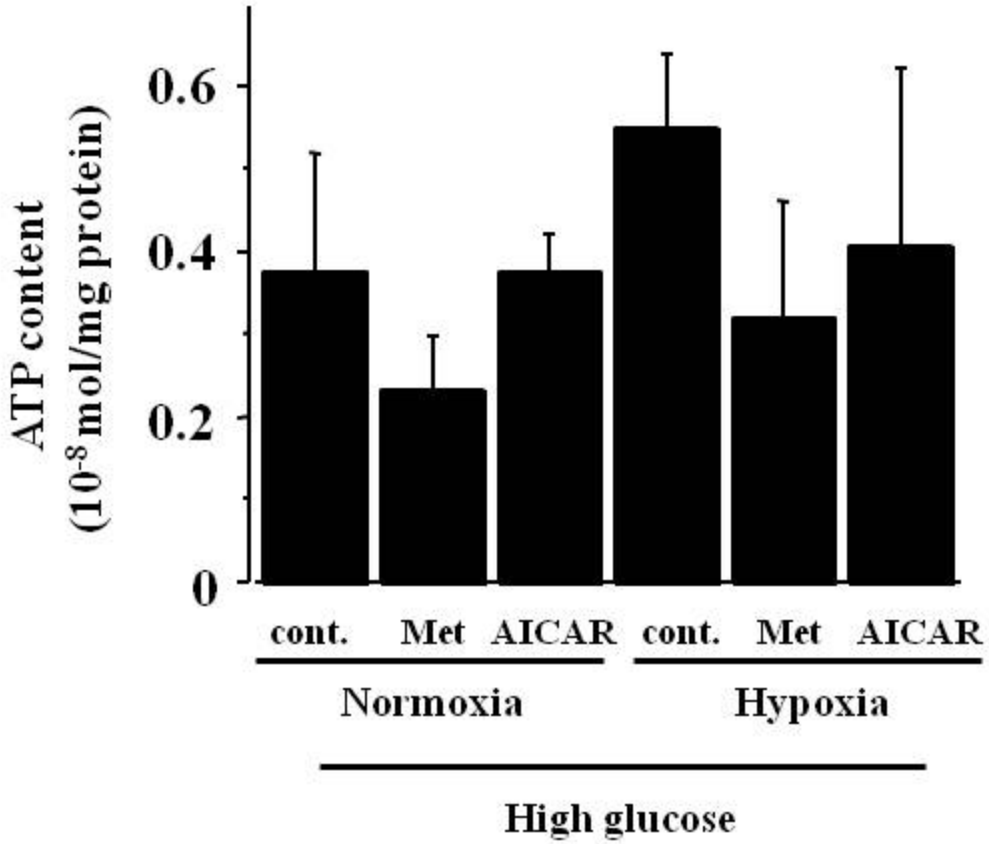
ATP content
(10-8 mol/mg protein)
0.6
0.4
0.2
0
cont.
Met
AICAR
cont.
Met
AICAR
Normoxia
Hypoxia
High glucose

Figure 4.

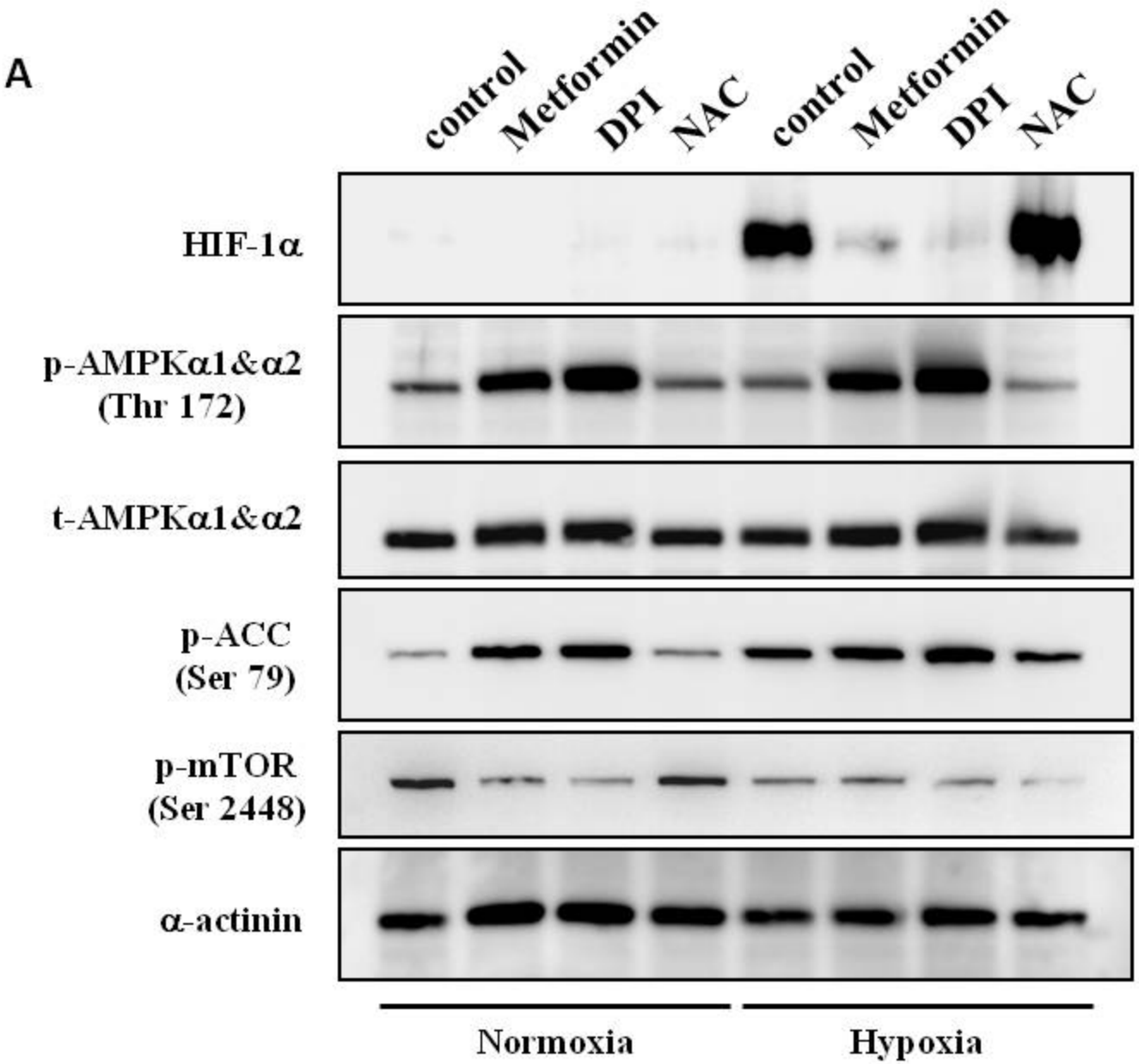
A
control
Metformin
DPI
NAC
control
Metformin
DPI
NAC
HIF-1α
p-AMPKα1&α2
(Thr 172)
t-AMPKα1&α2
p-ACC
(Ser 79)
p-mTOR
(Ser 2448)
α-actinin
Normoxia
Hypoxia

Figure 5.

B

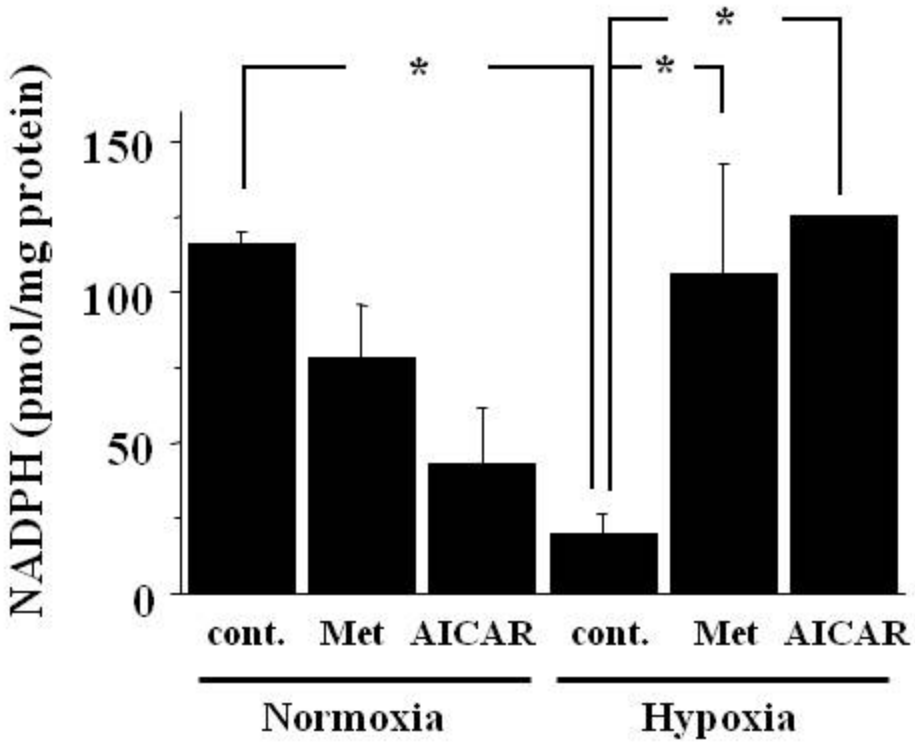
NADPH (pmol/mg protein)
150
100
50
0
*
*
*
cont.
Met
AICAR
cont.
Met
AICAR
Normoxia
Hypoxia

Figure 5.

C

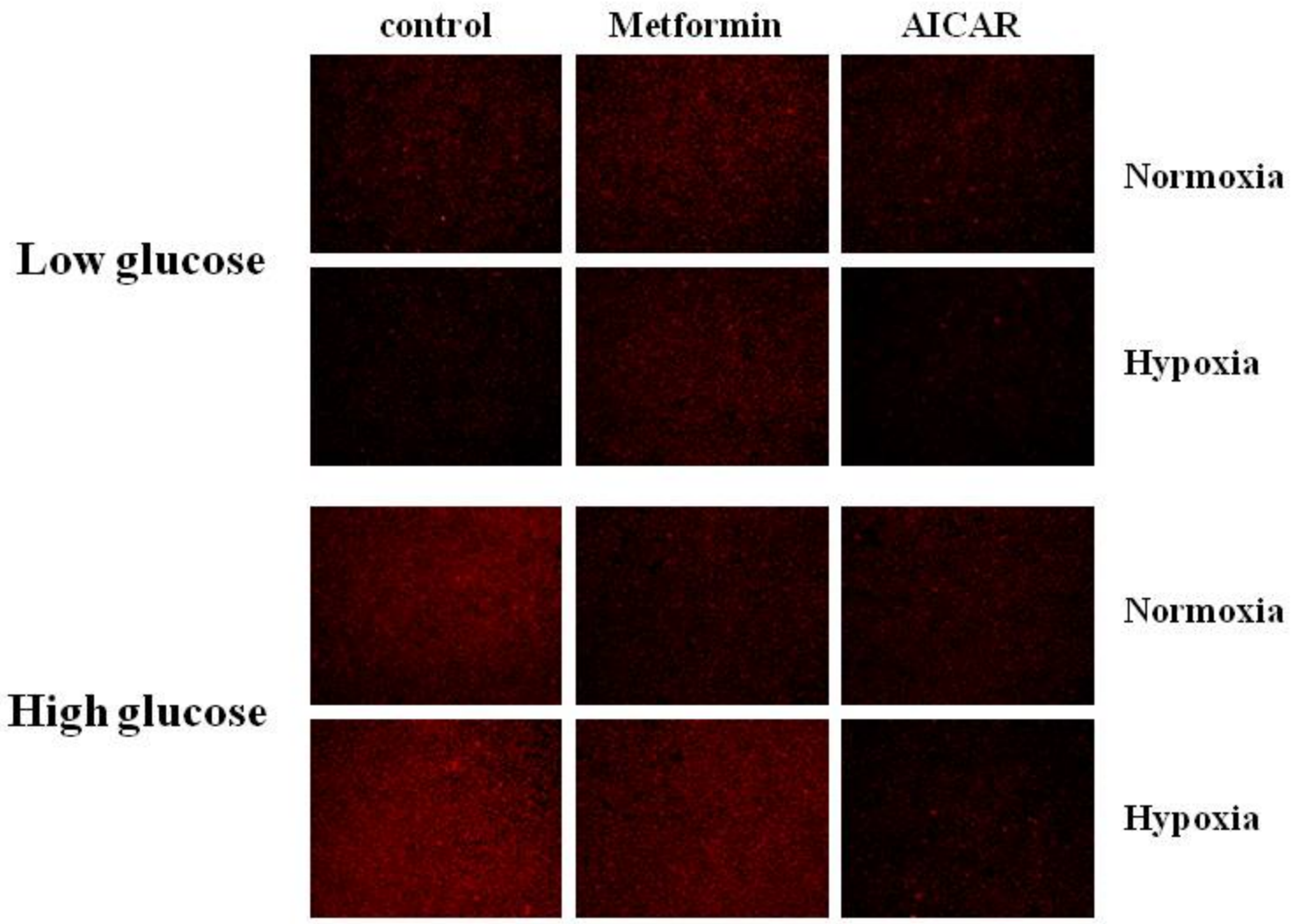
control
Metformin
AICAR
Low glucose
High glucose
Normoxia
Hypoxia
Normoxia
Hypoxia

Figure 5.

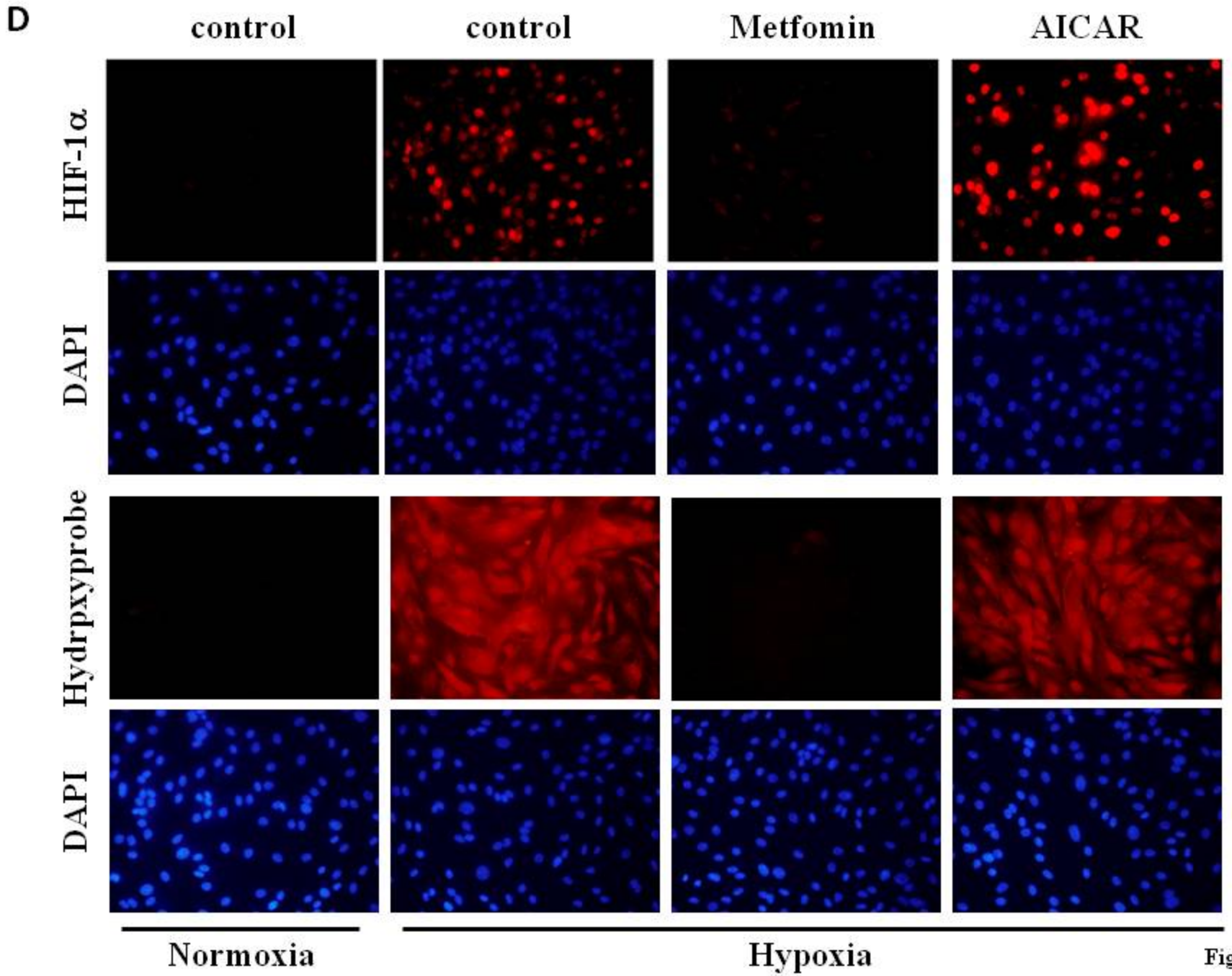
D
control
control
Metfomin
AICAR
HIF-1α
DAPI
Hydrpxyprobe
DAPI
Normoxia
Hypoxia

Figure 5.

A

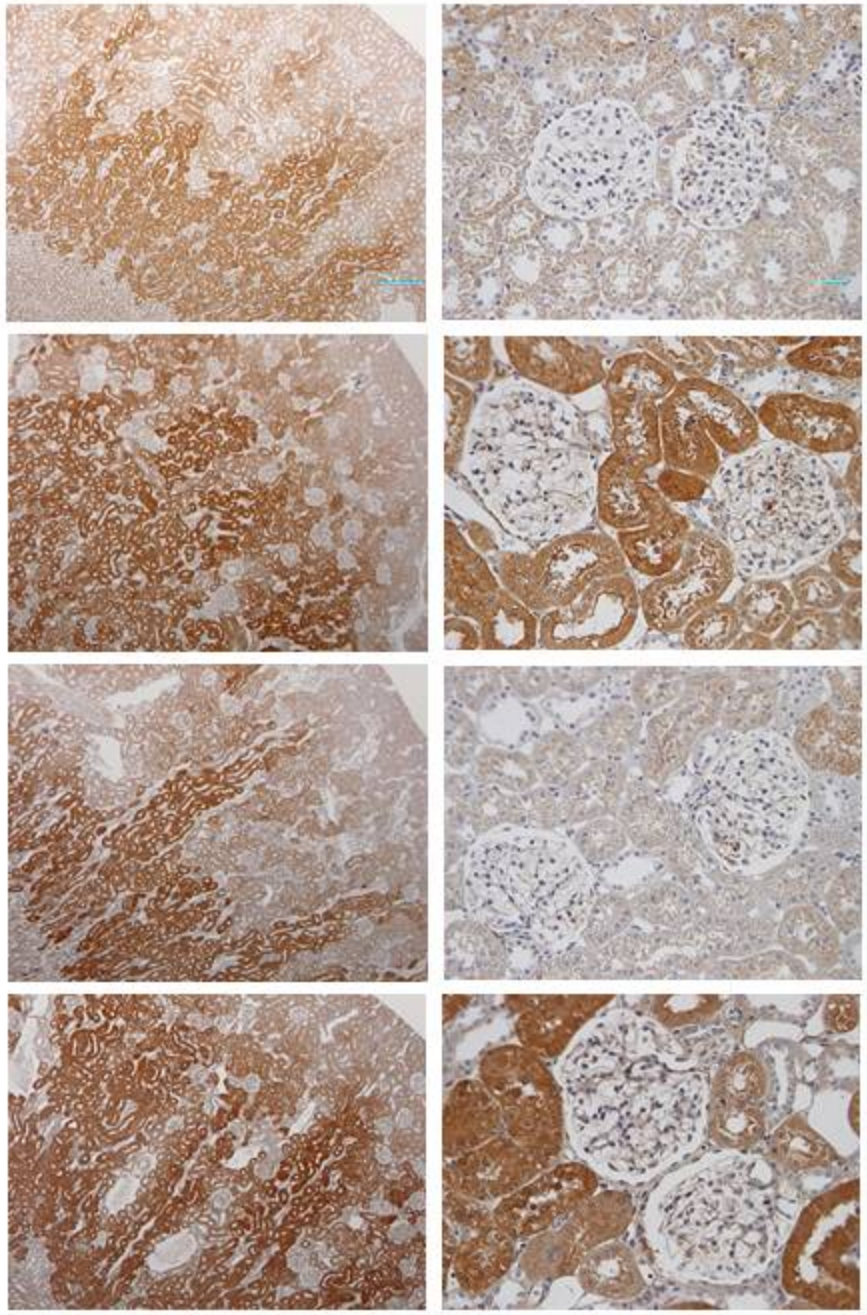

Figure 6.

B

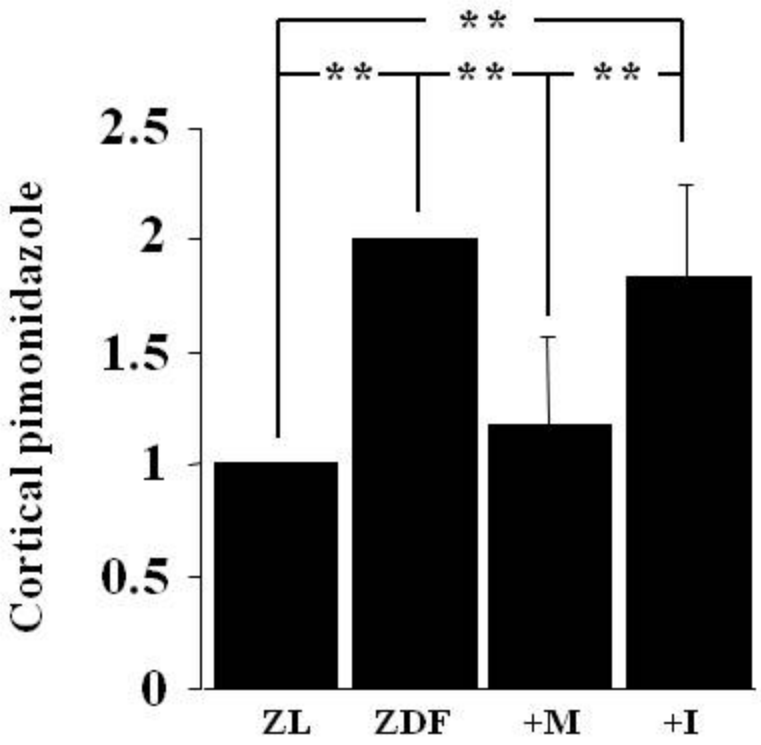

Figure 6.

C

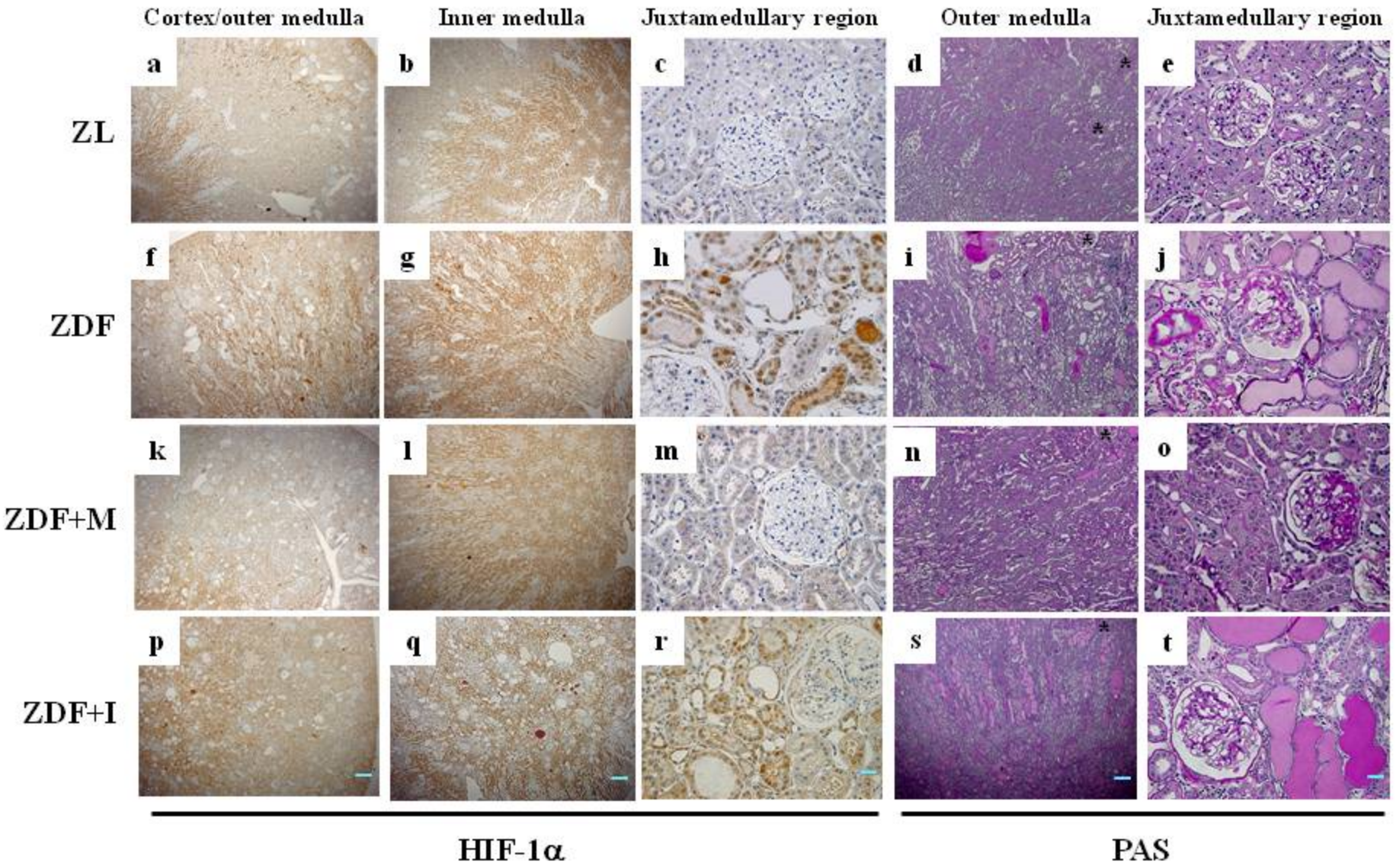
Cortex/outer medulla
Inner medulla
Juxtamedullary region
Outer medulla
Juxtamedullary region
ZL
ZDF
ZDF+M
ZDF+I
a
b
c
d
e
f
g
h
i
j
k
l
m
n
o
p
q
r
s
t
HIF-1α
PAS

Figure 6.

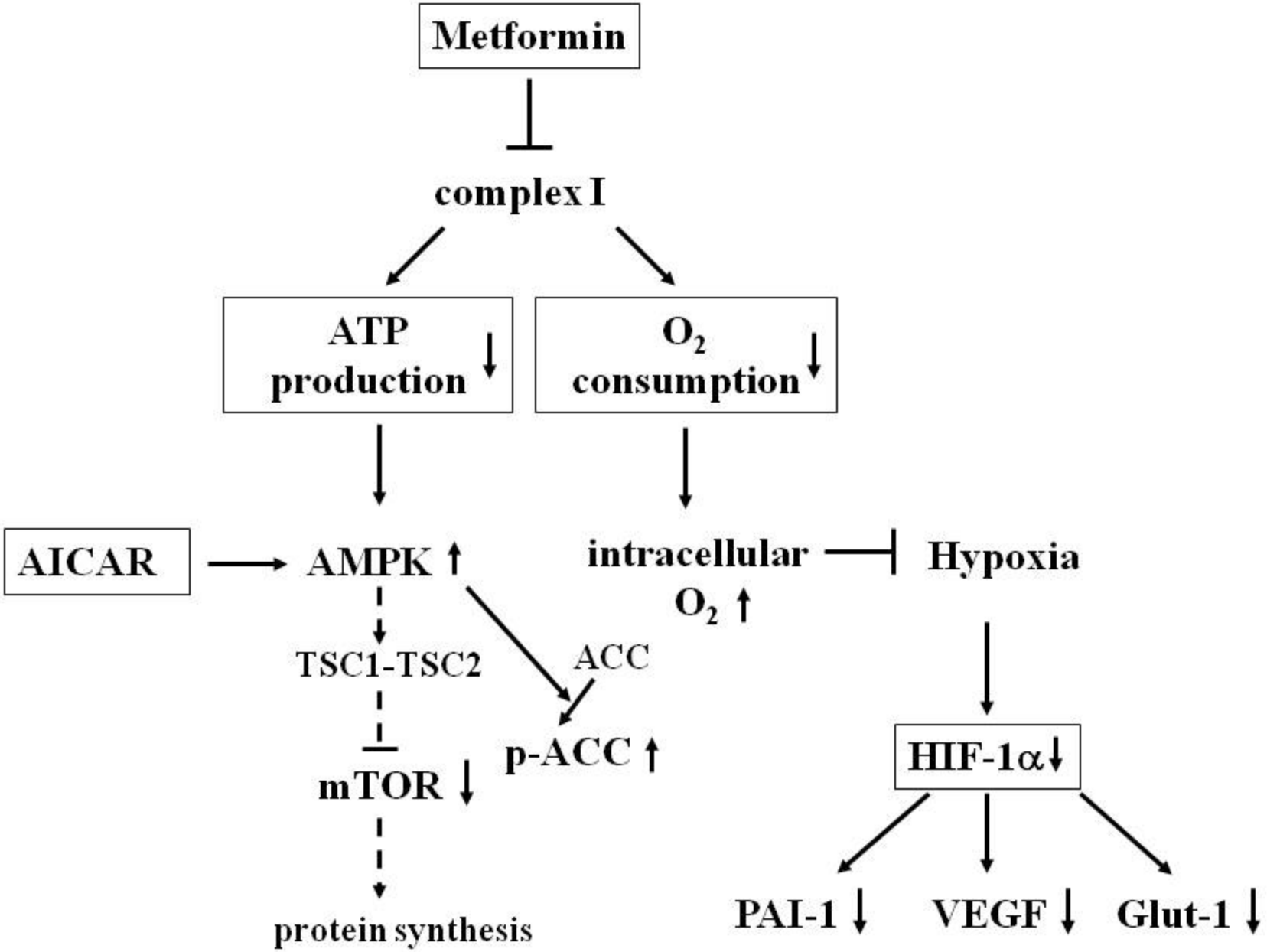
Metformin
complex I
ATP production ↓
O_2 consumption ↓
AICAR
AMPK ↑
intracellular O_2 ↑
Hypoxia
TSC1-TSC2
ACC
p-ACC ↑
mTOR ↓
protein synthesis
HIF-1α↓
PAI-1 ↓
VEGF ↓
Glut-1 ↓

Figure 7.